Chemical Geology 385 (2014) 35–55

Contents lists available at ScienceDirect

Chemical Geology

journal homepage: www.elsevier.com/locate/chemgeo

Sr and Nd isotopic compositions of apatite reference materials used in U–Th–Pb geochronology

Yue-Heng Yang [a,*], Fu-Yuan Wu [a], Jin-Hui Yang [a], David M. Chew [b], Lie-Wen Xie [a], Zhu-Yin Chu [a], Yan-Bin Zhang [a], Chao Huang [a]

[a] State Key Laboratory of Lithospheric Evolution, Institute of Geology and Geophysics, Chinese Academy of Sciences, P. O. Box 9825, Beijing 100029, China
[b] Department of Geology, School of Natural Sciences, Trinity College Dublin, Dublin 2, Ireland

ARTICLE INFO

Article history:
Received 9 October 2013
Received in revised form 11 July 2014
Accepted 11 July 2014
Available online 19 July 2014

Editor: L. Reisberg

Keywords:
Apatite
Sr isotopes
Sm–Nd isotopes
LA-MC-ICP-MS
U–Th–Pb geochronology

ABSTRACT

Apatite is an important common U- and Th-bearing accessory mineral in igneous, metamorphic and clastic sedimentary rocks. The advent of *in situ* U–Th–Pb apatite geochronology by the SIMS and LA-(MC)-ICP-MS methods has demonstrated the importance of having uniform and homogeneous reference materials. Recently, it has been shown that Sr and Nd isotopic data combined with U–Pb age and trace element concentration data can provide important constraints on apatite paragenesis because this phase usually exhibits high Sr and REE concentrations but has low Rb/Sr ratios which result in negligible corrections for the ingrowth of radiogenic Sr. However, as apatite can potentially have complex internal structures resulting from multiple thermal events, such as inherited cores and metamorphic overgrowths, requires that the Sr and Nd isotopic data should be measured with high spatial resolution. However isobaric interferences hamper the precise determination of Sr or Nd isotopic compositions in LA-MC-ICP-MS analysis. In this work we undertook *in situ* measurements of Sr and Nd isotopic compositions of eleven apatite reference materials (AP1, AP2, Durango, MAD, Otter Lake, NW-1, Slyudyanka, UWA-1, Mud Tank, McClure Mountain and SDG) commonly used in U–Th–Pb geochronology. Our obtained Sr and Sm–Nd isotopic compositions for these apatite samples are consistent with those values obtained by solution-based methods (isotope dilution and ion chromatography) using MC-ICP-MS or TIMS, which demonstrates the reliability and robustness of our analytical protocol.

1. Introduction

Apatite [$Ca_5(PO_4)_3(F,OH,Cl)$] is a minor but ubiquitous mineral in diverse terrestrial and lunar rocks (Pan and Fleet, 2002; Poitrasson et al., 2002), and its major- and trace element compositions have been widely used in petrogenetic and mineral exploration studies (*e.g.* Sha and Chappell, 1999; Belousova et al., 2001, 2002; Chu et al., 2009a). It is becoming increasingly used in *in situ* U–Pb geochronology studies (Sano et al., 1999, 2006; Chew et al., 2011; Li et al., 2012; Thomson et al., 2012; Chew et al., 2014), while it has been long recognized that apatite can also provide important Sr–Nd isotopic petrogenetic information (Zaitsev and Bell, 1995; Rakovan et al., 1997). Typically its $^{87}Sr/^{86}Sr$ composition can be regarded as the initial strontium isotopic value because of the extremely low Rb/Sr ratio in most apatites (normally $^{87}Rb/^{86}Sr < 0.0001$). Recent developments in *in situ* laser ablation techniques make it possible to determine rapidly Sr (Bizzarro et al., 2003; Schmidberger et al., 2003; Horstwood et al., 2008; Nowell and Horstwood, 2009; Yang et al., 2009a,b; Henderson et al., 2010; Wu et al., 2010a,b,c; Mitchell et al., 2011; Wu et al., 2011, 2013a,b) or Nd (Foster and Vance, 2006; Foster and Carter, 2007; McFarlane and McCulloch, 2007, 2008; Yang et al., 2008; Carter and Foster, 2009; Gregory et al., 2009; Wu et al., 2010a,b,c; Mitchell et al., 2011; Wu et al., 2011, 2013a,b) isotopic compositions. Additionally, apatite has also been used to construct precise Lu–Hf isochrons due to its high Lu/Hf ratio (Scherer et al., 2001; Barfod et al., 2002, 2003, 2005; Soderlund et al., 2004; Amelin, 2005). It is increasingly recognized that apatite has wide applications in the Earth sciences, including geochronology, isotopic tracing and geochemical discrimination studies. Combined, these approaches can provide invaluable petrogenetic information.

Multi-collector thermal ionization mass spectrometry (TIMS) is still regarded as the benchmark method for Sr or Nd isotopic analysis owing to its inherent high precision (*e.g.* Li et al., 2007; Chu et al., 2009b). Nevertheless, this technique is significantly more time consuming compared to micro-beam methods (*e.g.* SIMS or LA-ICP-MS). Additionally the TIMS method is unable to detect spatial variations in isotopic compositions unless micro-drilling is employed. Recently, multi-collector inductively coupled plasma mass spectrometry (MC-ICP-MS) has become a routine tool for Sr or Nd isotopic measurements with the advantage of high sample throughput (Ehrlich et al., 2001; Waight et al., 2002; Fortunato et al., 2004; Balcaen et al., 2005; Yang et al., 2011c).

* Corresponding author. Tel.: +86 10 82998599; fax: +86 10 62010846.
E-mail address: yangyueheng@mail.iggcas.ac.cn (Y.-H. Yang).

http://dx.doi.org/10.1016/j.chemgeo.2014.07.012
0009-2541/

Additionally, when coupled to laser ablation (LA) systems, *in situ* MC-ICP-MS analysis makes it possible to obtain rapidly Sr or Nd isotopic data from Sr- or REE-enriched minerals. While the precision of Sr or Nd data obtained by LA-MC-ICP-MS cannot compare with that of TIMS, sample preparation is much easier and the sample throughput is significantly higher (*e.g.* Adams et al., 2005; Hart et al., 2005; Jackson and Hart, 2006; Balter et al., 2008; Copeland et al., 2008; Fietzke et al., 2008; Richards et al., 2008; Simonetti et al., 2008; Vroon et al., 2008; Richards et al., 2009; Copeland et al., 2010; Yang et al., 2011a; Guo et al., 2014; Yang et al., 2014a).

Similar to *in situ* Hf isotopic analyses on zircon (Woodhead and Hergt, 2005; Wu et al., 2006; Blichert-Toft, 2008; Fisher et al., 2011a) or *in situ* Pb isotopic analyses on K-feldspar (Tyrrell et al., 2006), matrix-matched reference materials are required for *in situ* Sr or Nd analyses (Yang et al., 2009a; Wu et al., 2010a,b,c). Undoubtedly, some apatite reference materials employed in U–Th–Pb geochronology studies using the SIMS or LA-MC-ICP-MS techniques have potential as *in situ* Sr or Nd reference materials. Nevertheless, their suitability as apatite Sr or Nd reference materials has not been investigated in detail, with only a few Sr and Nd isotopic data available for Durango apatite (Foster and Vance, 2006; McFarlane and McCulloch, 2008; Fisher et al., 2011b; Hou et al., 2013; Kimura et al., 2013a,b). Other apatite reference materials (*e.g.* AP1, AP2, MAD, Otter Lake, NW-1, Slyudyanka, UWA-1, Mud Tank, McClure Mountain and SDG) have not been investigated for their Sr and Nd isotopic compositions, although their U–Th–Pb age systematics have been well characterized using SIMS (Sano et al., 1999; Nishizawa et al., 2004; Frei et al., 2005; Sano et al., 2006; Li et al., 2012), LA-ICP-MS (Chew et al., 2011, 2014) or LA-(MC)-ICP-MS (Willigers et al., 2002; Thomson et al., 2012). Therefore, more data and inter-laboratory comparisons are required to evaluate the suitability of apatite age reference materials as potential Sr or Nd reference materials.

In this paper, we first present our Sr and Nd isotopic analyses for MAD, Otter Lake, NW-1, Slyudyanka, Durango, UWA-1, Mud Tank, McClure Mountain and SDG apatite using both solution-based and laser-ablation sampling techniques in our laboratory. Additionally, the suitability of two gem quality apatite megacrysts (AP1 and AP2), probably from Madagascar, was also evaluated for use as our *in-house* Sr or Nd apatite reference materials. The Sr and Nd isotopic compositions obtained for these natural apatite samples are all consistent with values obtained by solution-based methods (isotope dilution and ion chromatography) using MC-ICP-MS or TIMS, which indicates the reliability and robustness of our analytical protocol.

2. Analytical methods

All eleven apatite samples investigated in this work were embedded in epoxy resin blocks and polished prior to being analyzed for their major and trace element concentrations and their Sr and Nd isotopic compositions using *in situ* techniques. To validate the reliability of the *in situ* analyses, the Sr and Nd isotopic compositions of aliquots of the eleven apatite reference materials were also analyzed by ID-TIMS or ID-MC-ICP-MS. All analyses were conducted at the State Key Laboratory of Lithospheric Evolution, the Institute of Geology and Geophysics, Chinese Academy of Sciences, Beijing.

2.1. Major and trace element analyses

Major element analyses were conducted by electron microprobe analysis (EMPA) using a JEOL–JAX8100. The typical beam size was 20 μm and an accelerating voltage of 15 kV and a beam current of 20 nA were employed. Counting times were 20 s and total Fe is expressed as Fe_2O_3. Analyses were acquired using the Probe for Windows software and X-ray correction was undertaken using the CITZAF software. The analytical uncertainties are within 2% for TiO_2 and CaO, but are ~10–20% for other elements due to their low concentrations.

In situ trace element concentration analyses of individual apatite grains were conducted using an Agilent 7500a quadruple inductively coupled plasma mass spectrometer (Q-ICP-MS) coupled to a 193 nm excimer ArF laser ablation system. The analytical protocol employed is similar to that outlined in Xie et al. (2008). Helium gas was flushed to minimize aerosol deposition around the ablation site, and mixed with argon gas downstream of the ablation cell. During analysis, a spot size of 30 μm was applied with a repetition rate of 6 Hz, and the energy density employed was ~10 J/cm^2. All measurements were performed in time-resolved analysis mode utilizing peak jumping with 1 point per mass peak. Each spot analysis consisted of approximately 30 s of background acquisition and 60 s of sample data acquisition. Every five sample analyses were followed by one NIST SRM 610 measurement. Raw counts were processed offline and data-reduction and concentration calculations were then performed using the Glitter laser ablation software (Griffin et al., 2008). For calibration purposes, Ca determined by electron microprobe, was used as an internal standard.

2.2. In situ Sr isotopic analyses

In situ Sr isotopic measurements by MC-ICP-MS have already been described in detail elsewhere (Yang et al., 2009b), hence only a brief description is given below. A spot size of 60–120 was employed with a 6–8 Hz repetition rate and an energy density of 10 J/cm^2, depending on the Sr concentration of the samples. The Sr isotopic data were acquired by static multi-collection in low-resolution mode using nine Faraday collectors. Prior to laser analyses, the Neptune MC-ICP-MS was tuned using a standard solution to obtain maximum sensitivity. A typical data acquisition cycle consisted of a 40 s measurement of the Kr gas blank with the laser switched off, followed by 60 s of measurement with the laser ablating. As will be discussed below, AP1 has a nearly uniform Sr isotopic composition. Every ten sample analyses were followed by one AP1 apatite reference material measurement for external calibration. Meanwhile, AP2 apatite was analyzed in each analytical session and treated as an unknown sample during the data-reduction procedure.

Data reduction was done offline and the potential isobaric interferences were accounted for in the following order: Kr, Yb^{2+}, Er^{2+} and Rb. Firstly, the interference of ^{84}Kr and ^{86}Kr on ^{84}Sr and ^{86}Sr, respectively, was removed using the 40 s Kr gas baseline measurement. The isobaric interference correction of ^{84}Kr and ^{86}Kr on ^{84}Sr and ^{86}Sr was conducted using the natural Kr isotopic ratios ($^{83}Kr/^{84}Kr = 0.20175$, $^{83}Kr/^{86}Kr = 0.66474$) (Christensen et al., 1995; Bizzarro et al., 2003). Secondly, the presence of $^{167}Er^{2+}$, $^{171}Yb^{2+}$ and $^{173}Yb^{2+}$ at masses 83.5, 85.5 and 86.5 was monitored based on the protocols of Ramos et al. (2004). Using the isotopic abundances of Er and Yb (Chartier et al., 1999), the potential double-charged ion isobaric interference of $^{166}Er^{2+}$ (at m/z 83), $^{168}Er^{2+}$ (at m/z 84) and $^{170}Er^{2+}$ (at m/z 85) on $^{83}Kr^{+}$, $^{84}Sr^{+}$ and $^{85}Rb^{+}$, respectively, was evaluated and corrected by monitoring the interference-free $^{167}Er^{2+}$ (at m/z 83.5) signal intensity. Similarly, the potential double-charged ion isobaric interference of $^{170}Yb^{2+}$ (at m/z 85), $^{172}Yb^{2+}$ (at m/z 86), $^{174}Yb^{2+}$ (at m/z 87) and $^{176}Yb^{2+}$ (at m/z 88) on $^{85}Rb^{+}$, $^{86}Sr^{+}$, $^{87}Sr^{+}$ and $^{88}Sr^{+}$, respectively, was assessed and corrected for by monitoring the interference-free $^{173}Yb^{2+}$ (at m/z 86.5) signal intensity (Yang et al., 2014b). Thirdly, the natural ratio of $^{85}Rb/^{87}Rb$ (2.5926) was used to correct for isobaric interference of ^{87}Rb on ^{87}Sr by the exponential law, assuming that Rb has the same mass discrimination behavior as Sr (Christensen et al., 1995; Ehrlich et al., 2001; Bizzarro et al., 2003; Ramos et al., 2004, 2005; Woodhead et al., 2005; Richards et al., 2008; Yang et al., 2011a, 2012). It is observed that the obtained $^{87}Rb/^{87}Sr$ ratio is typically less than 0.0005 during *in situ* apatite Sr analysis, indicating that the radiogenic ^{87}Sr contribution is negligible (Yang et al., 2011a). In addition, our previous work demonstrated that Ca argides and dimers had an insignificant influence on Sr isotope analysis using a Neptune MC-ICP-MS (Yang et al., 2011c), a conclusion that is also strongly supported by other studies (Bizzarro et al., 2003; Ramos et al., 2004; Yang

et al., 2011a). A polyatomic interference by Ca–P–O has also been documented in *in situ* Sr analysis studies by LA-MC-ICP-MS (*e.g.* Horstwood et al., 2008). However, this interference is most significant for low Sr contents such as in tooth enamel (<300 ppm Sr, Horstwood et al., 2008; Nowell and Horstwood, 2009 and Figs. 3, 4 & 5 therein). In this study, the Sr concentration of the apatite reference materials is usually more than 1000 ppm and so the potential effect of a Ca–P–O polyatomic interference would be significantly less, a conclusion which is also supported by other studies (Copeland et al., 2010). Additionally, there is no systematic offset in this study between the Sr isotopic data obtained by LA-MC-ICP-MS and the Sr isotopic data on the same samples determined by solution-based methods (which employed ion chromatography to elute away matrix elements such as Ca and P). Therefore, interferences from Ca argides or dimers and Ca–P–O are not considered further in this work. Finally, the $^{87}Sr/^{86}Sr$ ratios were calculated and normalized from the interference-corrected $^{86}Sr/^{88}Sr$ ratio using the exponential law. The whole data-reduction procedure was performed using an in-house Excel VBA (Visual Basic for Applications) macro program.

2.3. In situ Nd isotopic analyses

The protocol for *in situ* Nd isotopic analysis has been described in detail elsewhere (Yang et al., 2008; Liu et al., 2012) and is described briefly below. Prior to laser analyses, the Neptune MC-ICP-MS was tuned and optimized for maximum sensitivity using JNdi-1 standard solution. A laser spot size of 60–120 μm was employed with a 6–8 Hz repetition rate, depending on the Nd concentration of the samples. Each spot analysis consisted of approximately 60 s data acquisition with the laser fired on. As will be discussed below, AP2 has a nearly uniform Nd isotopic composition. Every ten sample analyses were followed by one AP2 apatite reference material measurement for external calibration. Meanwhile, AP1 apatite was analyzed in each analytical session and treated as an unknown during the data-reduction protocol.

In order to obtain accurate $^{147}Sm/^{144}Nd$ and $^{143}Nd/^{144}Nd$ apatite data by LA-MC-ICP-MS, great care must be taken to adequately correct for the contribution of the isobaric interference of ^{144}Sm on the ^{144}Nd signal. The Sm interference correction is complicated by the fact that the $^{146}Nd/^{144}Nd$ ratio, which is conventionally used to normalize the other Nd isotope ratios, is also affected by Sm interference. As a result the mass bias correction of ^{144}Sm interference on ^{144}Nd cannot be applied directly from the measured $^{146}Nd/^{144}Nd$ ratio (Jackson et al., 2001; Foster and Vance, 2006; McFarlane and McCulloch, 2007, 2008; Yang et al., 2008, 2009a; Wu et al., 2010a,b,c; Yang et al., 2010a; Fisher et al., 2011b; Iizuka et al., 2011; Mitchell et al., 2011).

In this work, we present an approach similar to that of McFarlane and McCulloch (2007, 2008). However, we have adopted the recently revised Sm isotopic abundances ($^{147}Sm/^{149}Sm = 1.08680$ and $^{144}Sm/^{149}Sm = 0.22332$) (Dubois et al., 1992; Isnard et al., 2005). First, we used the measured $^{147}Sm/^{149}Sm$ ratio to calculate the Sm fractionation factor and the measured ^{147}Sm intensity by employing the natural $^{147}Sm/^{144}Sm$ ratio of 4.866559 (Isnard et al., 2005) to estimate the Sm interference on mass 144. The interference-corrected $^{146}Nd/^{144}Nd$ ratio can then be used to calculate the Nd fractionation factor. Finally, the $^{143}Nd/^{144}Nd$ and $^{145}Nd/^{144}Nd$ ratios were normalized using the exponential law (Yang et al., 2008, 2010a; Fisher et al., 2011b; Iizuka et al., 2011; Liu et al., 2012; Yang et al., 2013). The $^{147}Sm/^{144}Nd$ ratio of unknown samples can also be calculated using the exponential law after correcting for the isobaric interference of ^{144}Sm on ^{144}Nd as described above. The $^{147}Sm/^{144}Nd$ ratio was then externally further calibrated against the $^{147}Sm/^{144}Nd$ ratio of an AP2 apatite reference material during the analytical sessions (McFarlane and McCulloch, 2007, 2008; Iizuka et al., 2011; Liu et al., 2012; Yang et al., 2013). The raw data were exported offline and the whole data-reduction procedure was performed using an in-house Excel VBA (Visual Basic for Applications) macro program.

2.4. Sr–Nd isotopic analyses by solution-based methods

Apatite chemical purification was undertaken using conventional ion exchange chromatography (Yang et al., 2010b, 2011b). All chemical preparation was conducted on class 100 workbenches within a class 1000 over-pressured clean laboratory. Apatite crystal chips were washed in an ultrasonic bath with Milli-Q H_2O and then washed for several minutes with 2% HNO_3. About ~5–8 mg of apatite crystal was weighed into a 7 mL round bottom Savillex™ Teflon/PFA screw-top capsule. Weighed aliquots of ^{84}Sr or mixed ^{149}Sm–^{150}Nd isotopically enriched tracer were added to the samples followed by 3 mL of concentrated HCl. The capsules were capped and then heated on a hotplate at about 120 °C for five days. Following complete dissolution and spike-sample homogenization, the capsule was opened and then heated to evaporate to dryness. One mL of 6 M HCl was added to the residue and then evaporated. This procedure was performed twice. After cooling, the sample was dissolved in 1.5 mL of 2.5 M HCl. The capsule was again sealed and placed on a hot plate at about 100 °C overnight prior to chemical purification.

After centrifuging, the solution was loaded onto a quartz ion exchange column (*ca.* 100 × 5 mm) packed with 2 mL AG50W-X12 resin, pre-conditioned with 25 mL 6 M HCl and 2 mL of 2.5 M HCl, respectively. The resin was then washed with a further 2 mL of 2.5 M HCl, followed by 2.5 mL of 5 M HCl to remove undesirable matrix elements. Rb was then eluted with 1.5 mL of 5 M HCl. To minimize the potential isobaric interference of ^{87}Rb on ^{87}Sr and the resin was rinsed with 4 mL of 5 M HCl to remove any residual Rb. Finally, the Sr fraction was collected with 3 mL 5 M HCl and gently evaporated to dryness. Finally, the REE fraction was eluted and collected with 10 mL 6 M HCl (Li et al., 2007; Chu et al., 2009b; Yang et al., 2010b). The Nd and Sm separation was performed using Eichrom Ln resin (100–150 μm, 2 mL) with 0.25 M HCl used to elute Nd and 0.40 M HCl used to elute Sm, modified from the technique of Pin and Zalduegui (1997).

Additionally, in order to eliminate doubly charged ion (HREE) interference on Sr (Waight et al., 2002; Yang et al., 2012), all eluted Sr fractions from the standard cation resin were further purified using Sr-spec resin prior to TIMS or MC-ICP-MS measurements. Considering the strong retention of Sr on Sr-spec resins, the Sr fraction was dissolved in 1 mL of 3.0 M HNO_3 and the sample solution was loaded onto a Bio-Rad polypropylene column newly packed with 0.2 mL Sr-spec resin (Waight et al., 2002; Balcaen et al., 2005; Yang et al., 2012, 2014b). Subsequently, the resin was rinsed with 20 mL of 3 M HNO_3 and the Sr was stripped from the column using a small volume of 0.05 M HNO_3. The first milliliter was discarded and the next 5 mL was collected and dried down and then re-dissolved with 2–5 mL of 2% HNO_3 prior to analysis. A new portion of Sr-spec resin was used for each set of analyses.

Sr and Sm–Nd isotopic compositions were measured using a GV Instruments Isoprobe-T TIMS, and a Thermo Fisher Scientific TRITON Plus TIMS and Neptune MC-ICP-MS (Li et al., 2007; Chu et al., 2009b; Yang et al., 2011b, 2011c, 2012). The total procedural blanks were less than 100 pg for Sr and 50 pg for Sm and Nd, indicating a negligible blank contribution and hence no correction was applied to the measured isotopic ratios. $^{87}Sr/^{86}Sr$ and $^{143}Nd/^{144}Nd$ ratios were normalized to $^{86}Sr/^{88}Sr = 0.1194$ and $^{146}Nd/^{144}Nd = 0.7219$ respectively, using the exponential law. During the period of data acquisition, standard reference material analyses yielded results of $^{87}Sr/^{86}Sr = 0.710250 \pm 11$ (2SD, n = 18) for NBS987 and $^{143}Nd/^{144}Nd = 0.512110 \pm 12$ (2SD, n = 16) for JNdi-1. In addition, the USGS reference materials BCR-2 and BHVO-2 yielded results of 0.705002 ± 12 ($2\sigma_m$) and 0.703489 ± 11 ($2\sigma_m$) for $^{87}Sr/^{86}Sr$, 0.512636 ± 10 ($2\sigma_m$) and 0.512995 ± 15 ($2\sigma_m$) for $^{143}Nd/^{144}Nd$ and 0.1385 and 0.1096 for $^{147}Sm/^{144}Nd$ respectively, which is identical within error to their published values (Weis et al., 2006).

3. Results

To date there are no reported Sr or Nd isotopic data for these apatite reference materials in the literature with the exception of Durango apatite. Their major and trace element concentrations and their Sr and Nd isotopic data (obtained by LA-MC-ICP-MS) are summarized in Tables 1, 2 and 3 respectively. REE and multi-element diagrams ("spidergrams") are presented in Fig. 1. Additionally, Sr and Nd isotopic data on apatite crystal chips obtained by isotope dilution and ion chromatography followed by analysis by TIMS or MC-ICP-MS are shown in Table 4 for comparison.

3.1. AP1 and AP2 apatites

As noted previously, two gem quality apatites AP1 and AP2 (1.5 cm × 1 cm × 0.5 cm, unknown location, probably from Madagascar) are used as in-house apatite reference materials in our laboratory for laser ablation Sr and Nd isotopic analyses (Yang et al., 2008, 2009a). ID-TIMS analyses yielded a common Pb-corrected $^{206}Pb/^{238}U$ age of 475 Ma for both AP1 and AP2 apatite (Zhou, 2013). REE analyses by LA-ICP-MS indicate that AP1 and AP2 are LREE enriched and exhibit a weak negative Eu anomaly (Fig. 1a). AP1 exhibits higher Sr contents than AP2 (Fig. 1b).

A pilot suite of *in situ* LA-MC-ICP-MS analyses positioned on random locations across apatite AP1 indicated that this reference material has a uniform $^{87}Sr/^{86}Sr$ ratio (Fig. 2a). To confirm this finding, twelve separate fragments of the AP1 crystal were dissolved and separated using the ion chromatography methods described previously. The individual Sr isotopic results obtained by TIMS and MC-ICP-MS yield an average $^{87}Sr/^{86}Sr$ value of 0.711370 ± 31 (2SD, n = 14) (Table 4), which is the reference value used for externally calibrating other apatite reference materials during the *in situ* Sr isotope analytical sessions in this study. Our previous solution and laser analyses of apatite AP1 yielded $^{87}Sr/^{86}Sr$ values of 0.71138 ± 2 (2SD, n = 4) and 0.71137 ± 7 (2SD, n = 61), respectively (Yang et al., 2009b). Recently, Hou et al. (2013) reported an $^{87}Sr/^{86}Sr$ value of 0.71136 ± 9 (2SD, n = 16) for apatite AP1 by LA-MC-ICP-MS (Table 5).

Similarly, our data from the last six years indicate that AP1 apatite is relatively homogeneous in terms of its Nd isotopic composition (Fig. 2b). As shown in Table 3, the $^{143}Nd/^{144}Nd$ ratios from apatite AP1 range from 0.511340 ± 34 (2SD n = 14) to 0.511374 ± 34 (2 SD, n = 10) with an average value of 0.511349 ± 38 (2SD, n = 396), while the $^{147}Sm/^{144}Nd$ ratios range from 0.0813 ± 5 (2SD, n = 12) to 0.0831 ± 4 (2SD, n = 12) with an average value of 0.0822 ± 14 (2SD, n = 396). The mean $^{145}Nd/^{144}Nd$ value of 0.348410 ± 34 (2SD, n = 396) is consistent with the recommended value of 0.348415 (Wasserburg et al., 1981; Liu et al., 2012) (Table 3). For comparison, twelve different chips from a large crushed crystal of AP1 apatite were selected at random for solution MC-ICP-MS analyses (Table 4), yielding mean $^{143}Nd/^{144}Nd$ and $^{147}Sm/^{144}Nd$ ratios of 0.511352 ± 24 (2SD, n = 12) and 0.0825 ± 12 (2SD, n = 10), respectively (Fig. 2b). The corresponding $\varepsilon_{Nd(t)}$ average value for AP1 apatite is −18.2 ± 0.5 (2SD, n = 10) (Table 4), which is almost identical to the $\varepsilon_{Nd(t)}$ average value of −18.2 ± 0.8 (2SD, n = 396) obtained by the laser ablation technique (Table 3, Fig. 2b).

AP2 apatite yielded a homogenous $^{143}Nd/^{144}Nd$ and exhibited a narrow variation in $^{147}Sm/^{144}Nd$ ratio (RSD < 1%) during our laser ablation sessions (Fig. 2d) (Liu et al., 2012). Twelve separate chips of the apatite crystal AP2 were dissolved and analyzed and yielded average $^{143}Nd/^{144}Nd$ and $^{147}Sm/^{144}Nd$ ratios of 0.511007 ± 30 (2SD, n = 13) and 0.0764 ± 2 (2SD, n = 10), respectively (Table 4). The Nd isotopic composition of apatite AP2 is therefore homogeneous and it has been used to calibrate externally the other apatite samples during this study.

Table 1
Major (wt.%) and trace element (ppm) composition of the apatite reference materials in this study.

Sample	AP1	AP2	Durango Chew	Durango Fisher	Durango Griffin	Durango Hou	MAD	Otter Lake	NW-1	Slyudyanka	UWA-1	Mud Tank	McClure Mountain	SDG
SiO_2	0.79	1.22	0.46	0.18	0.32	0.28	0.83	0.94	1.25	0.44	0.97	0.01	0.25	3.04
FeO	0.02	0.01	0.03	0.04	0.04	0.03	0.02	0.02	0.01	0.01	0.00	0.07	0.01	0.00
MnO	0.03	0.03	0.02	0.01	0.01	0.01	0.02	0.01	0.02	0.02	0.02	0.03	0.03	0.02
MgO	0.00	0.01	0.04	0.02	0.02	0.03	0.01	0.00	0.01	0.01	0.01	0.06	0.01	0.01
CaO	55.57	55.66	53.90	53.99	53.85	53.94	55.30	53.44	54.24	54.66	53.67	55.30	55.08	51.58
SrO	0.24	0.07	0.05	0.04	0.05	0.05	0.17	0.20	0.53	0.14	0.10	0.35	0.40	1.44
P_2O_5	40.82	39.74	41.88	42.16	41.91	42.25	39.94	38.45	39.81	40.70	40.12	42.09	41.83	34.48
Cl	0.30	0.20	0.41	0.43	0.40	0.39	0.20	0.05	0.01	0.13	0.02	0.04	0.02	0.24
F	3.97	4.16	3.71	3.63	4.53	3.68	4.13	4.88	1.84	3.88	4.49	2.02	3.37	4.15
Total	100.01	99.30	99.21	99.44	99.54	99.44	98.83	96.58	96.96	99.58	97.42	99.33	99.59	93.21
Rb	0.18	0.26	0.12	0.11	0.13	0.12	0.25	0.43	0.15	0.02	0.44	0.22	0.12	0.20
Sr	2506	591	482	456	491	476	1650	1668	5512	1231	1186	2681	3422	11368
Ba	1.3	1.5	1.7	1.4	1.8	1.5	1.2	2	13	10	0.80	83	8.3	1.3
Nb	0.23	2.6	1.0	0.02	0.03	0.02	0.07	0.26	4.6	0.43	0.70	0.42	0.15	2.4
Ta	0.01	0.03	0.00	0.00	0.00	0.00	0.01	0.08	0.07	0.00	0.85	0.03	0.03	0.03
Zr	5.9	6.3	1.4	0.6	1.1	0.8	9.8	1.61	52	5.79	1.71	1.9	3.2	48
Hf	0.31	0.51	0.23	0.19	0.23	0.26	0.45	0.08	0.24	0.29	0.13	0.10	0.20	0.39
Pb	15	48	0.9	0.4	0.7	0.6	16	61	26	10	56	3.0	3.7	50
Th	647	2095	320	151	270	231	661	753	48	142	828	11	38	705
U	24	66	20	7	11	11	19	99	122	68	165	2.1	12	47
La	1925	2269	4285	3176	3819	3334	1745	2772	3576	77	2857	414	1609	7209
Ce	3783	4261	5405	3635	5178	4561	3338	6832	7477	140	6876	980	2362	15668
Pr	403	422	488	307	496	436	349	832	865	14	901	237	126	1843
Nd	1501	1435	1677	1009	1745	1514	1290	3205	3468	53	3747	550	843	7344
Sm	205	178	237	127	244	207	173	445	582	10	731	93	102	911
Eu	31	19	21	15	22	20	25	78	169	2	93	25	37	196
Gd	120	105	204	105	206	174	102	275	400	9	676	64	77	468
Tb	14	12	28	13	27	23	12	34	49	1	114	6.4	8.3	38
Dy	64	61	154	68	146	123	53	173	225	8	716	25	40	140
Ho	11	11	32	14	30	25	9.2	33	34	2	154	3.4	7.4	21
Er	25	26	83	34	77	64	21	85	68	5	421	6	18	49
Tm	3.0	3.3	10	4	10	8	2.4	11	7.0	1	55	0.5	2.3	5.5
Yb	18	20	59	27	56	47	15	68	35	4	311	2.4	14	33
Lu	2.3	2.4	6	4	7	6	1.9	8.4	3.6	0.48	31	0.25	1.9	4.3
Y	309	321	911	427	886	762	257	889	851	46	3583	73	206	605

Table 2
Laser ablation Sr isotopic analytical results of the apatite reference materials in this study.

Apatites	Analysis date	$^{84}Sr/^{86}Sr$ (±2SD)	$^{84}Sr/^{88}Sr$ (±2SD)	$^{87}Rb/^{86}Sr$ (±2SD)	$^{87}Sr/^{86}Sr$ (±2SD)	RSD (%)	Analyses Number
AP2	2009.09.14	0.0562(3)	0.00671(4)	0.0003(3)	0.72653(10)	0.014	35
AP2	2009.11.09	0.0561(4)	0.00669(5)	0.0005(3)	0.72649(09)	0.012	55
AP2	2010.10.14	0.0565(5)	0.00675(6)	0.0004(2)	0.72651(20)	0.027	14
AP2	2010.10.18	0.0561(8)	0.00670(10)	0.0003(2)	0.72656(16)	0.022	16
AP2	2010.10.19	0.0560(6)	0.00669(7)	0.0004(1)	0.72652(14)	0.019	10
AP2	2010.10.20	0.0562(3)	0.00671(4)	0.0004(1)	0.72661(19)	0.026	16
AP2	2010.10.21	0.0563(5)	0.00673(6)	0.0004(1)	0.72655(15)	0.020	19
AP2	2011.01.03	0.0560(4)	0.00669(5)	0.0005(3)	0.72660(13)	0.018	36
AP2	2011.02.22	0.0563(9)	0.00673(11)	0.0004(2)	0.72648(17)	0.024	14
AP2	2011.08.15	0.0559(5)	0.00668(6)	0.0007(6)	0.72656(14)	0.019	15
AP2	2011.08.17	0.0557(6)	0.00665(7)	0.0005(2)	0.72656(20)	0.027	13
AP2	2011.08.22	0.0563(6)	0.00673(8)	0.0005(7)	0.72657(16)	0.022	16
AP2	2011.08.23	0.0563(7)	0.00672(9)	0.0005(4)	0.72652(14)	0.019	38
AP2	2011.08.26	0.0565(8)	0.00675(9)	0.0004(2)	0.72659(18)	0.024	13
AP2	2011.08.29	0.0565(6)	0.00675(8)	0.0003(4)	0.72660(16)	0.022	16
AP2	**Mean**	**0.0562(7)**	**0.00671(8)**	**0.0004(4)**	**0.72655(16)**	**0.022**	**326**
Durango Hou	2009.11.06	0.0552(5)	0.00659(6)	0.0011(3)	0.70636(13)	0.018	15
Durango Hou	2009.11.07	0.0554(3)	0.00662(4)	0.0010(2)	0.70633(15)	0.022	11
Durango Hou	2009.11.08	0.0556(3)	0.00664(4)	0.0011(10)	0.70633(07)	0.010	13
Durango Hou	2010.10.14	0.0559(11)	0.00668(13)	0.0008(4)	0.70635(16)	0.022	18
Durango Hou	2010.10.15	0.0557(8)	0.00665(9)	0.0006(3)	0.70635(15)	0.021	11
Durango Hou	2010.10.18	0.0557(7)	0.00666(8)	0.0006(5)	0.70640(13)	0.018	16
Durango Hou	2010.10.21	0.0563(9)	0.00673(11)	0.0011(1)	0.70636(13)	0.018	17
Durango Hou	2011.01.03	0.0552(7)	0.00659(8)	0.0009(2)	0.70632(14)	0.019	55
Durango Hou	**Mean**	**0.0556(10)**	**0.00664(12)**	**0.0009(5)**	**0.70634(14)**	**0.020**	**156**
MAD	2011.08.12	0.0565(6)	0.00674(7)	0.0001(1)	0.71186(14)	0.020	20
MAD	2011.11.08	0.0566(4)	0.00676(5)	0.0000(1)	0.71179(06)	0.009	8
MAD	2011.11.09	0.0566(3)	0.00675(3)	0.0001(0)	0.71180(08)	0.012	15
MAD	2012.04.17	0.0565(7)	0.00675(8)	0.0002(2)	0.71179(08)	0.011	12
MAD	2012.04.18	0.0563(6)	0.00672(7)	0.0002(4)	0.71180(12)	0.017	13
MAD	2012.11.13	0.0565(3)	0.00675(3)	0.0001(0)	0.71177(09)	0.013	26
MAD	2012.11.14	0.0567(1)	0.00677(2)	0.0001(0)	0.71179(05)	0.007	18
MAD	**Mean**	**0.0565(5)**	**0.00675(6)**	**0.0001(2)**	**0.71180(11)**	**0.016**	**112**
Otter Lake	2011.08.12	0.0564(5)	0.00674(6)	0.0005(2)	0.70421(09)	0.013	20
Otter Lake	2011.11.08	0.0566(4)	0.00675(4)	0.0002(4)	0.70422(11)	0.015	21
Otter Lake	2011.11.09	0.0565(8)	0.00674(10)	0.0003(0)	0.70424(15)	0.021	9
Otter Lake	2012.04.17	0.0561(7)	0.00670(8)	0.0004(2)	0.70421(08)	0.012	15
Otter Lake	2012.04.18	0.0561(8)	0.00670(9)	0.0004(1)	0.70419(05)	0.007	8
Otter Lake	2012.11.13	0.0568(4)	0.00679(5)	0.0004(3)	0.70421(16)	0.022	26
Otter Lake	2012.11.14	0.0574(5)	0.00685(7)	0.0005(3)	0.70419(13)	0.018	19
Otter Lake	**Mean**	**0.0566(10)**	**0.00676(11)**	**0.0004(3)**	**0.70421(12)**	**0.017**	**117**
NW-1	2009.11.08	0.0565(4)	0.00674(5)	0.0001(1)	0.70246(07)	0.010	19
NW-1	2010.10.17	0.0564(2)	0.00674(3)	0.0001(1)	0.70249(07)	0.010	16
NW-1	2010.10.18	0.0564(2)	0.00674(3)	0.0002(9)	0.70248(05)	0.007	16
NW-1	2011.08.12	0.0564(5)	0.00674(5)	0.0001(0)	0.70249(09)	0.012	20
NW-1	2011.08.13	0.0564(4)	0.00673(5)	0.0001(0)	0.70249(12)	0.018	16
NW-1	**Mean**	**0.0564(4)**	**0.00674(4)**	**0.0001(4)**	**0.70248(08)**	**0.012**	**87**
Slyudyanka	2011.08.12	0.0566(4)	0.00676(4)	0.0000(0)	0.70769(11)	0.015	20
Slyudyanka	2011.11.08	0.0565(5)	0.00675(5)	0.0001(4)	0.70766(13)	0.018	20
Slyudyanka	2012.02.17	0.0565(6)	0.00675(7)	0.0001(4)	0.70770(15)	0.022	18
Slyudyanka	2012.02.18	0.0566(12)	0.00676(14)	0.0000(2)	0.70771(16)	0.023	18
Slyudyanka	2012.02.19	0.0563(7)	0.00672(8)	0.0002(12)	0.70766(13)	0.018	8
Slyudyanka	2012.11.16	0.0563(7)	0.00673(8)	0.0002(3)	0.70770(13)	0.018	15
Slyudyanka	2012.11.22	0.0565(8)	0.00674(9)	0.0001(1)	0.70773(21)	0.029	13
Slyudyanka	**Mean**	**0.0565(7)**	**0.00675(9)**	**0.0001(4)**	**0.70769(15)**	**0.021**	**110**
Mud Tank	2014.01.20	0.0563(4)	0.00673(5)	0.0000(0)	0.70302(08)	0.011	15
McClure Mountain	2014.01.20	0.0563(4)	0.00672(5)	0.0000(0)	0.70371(07)	0.011	13
SDG	2014.01.20	0.0564(7)	0.00673(8)	0.0000(0)	0.70298(16)	0.023	14

Bold data indicate the mean value of corresponding item for apatite reference materials.

Similarly, during the last three years, we obtained an $^{87}Sr/^{86}Sr$ ratio for apatite AP2 by LA-MC-ICP-MS of 0.72655 ± 16 (2SD, n = 326) (Fig. 2a), which is within uncertainty of the $^{87}Sr/^{86}Sr$ ratio of 0.72654 ± 5 (2SD, n = 13) obtained by solution-based methods (TIMS and MC-ICP-MS) (Table 4). The average $^{84}Sr/^{86}Sr$ and $^{84}Sr/^{88}Sr$ ratios obtained for apatite AP2 are 0.0562 ± 7 (2SD, n = 326) and 0.00671 ± 8 (2SD, n = 326) (Table 2), respectively, which are within error of the accepted values of 0.0565 and 0.00675 (Table 2). Additionally, our previous solution and laser analyses of apatite AP2 yielded $^{87}Sr/^{86}Sr$ values of 0.72655 ± 2 (2SD, n = 2) and 0.72652 ± 10 (2SD, n = 35), respectively (Yang et al., 2009b) (Table 5). Therefore, we chose to use AP1 as a Sr isotope external reference material and AP2 as a Nd isotope external reference material for the *in situ* apatite Sr and Nd isotopic analyses in this study.

3.2. Durango apatite

Durango apatite is a distinctive yellow-green fluorapatite that is found as exceptionally coarse crystals within the open pit iron mine at Cerro de Mercado, on the northern outskirts of Durango City, Mexico

Table 3
Laser ablation Nd isotopic analytical results of the apatite reference materials in this study.

Apatites	Analysis date	$[^{147}Sm/^{144}Nd]_m$ (±2SD)	RSD (%)	$[^{143}Nd/^{144}Nd]_m$ (±2SD)	$[^{145}Nd/^{144}Nd]_m$ (±2SD)	$[^{143}Nd/^{144}Nd]_i$	$\varepsilon_{Nd(t)}$ (±2SD)	Analyses Numbers
AP1	2007.09.30	0.0816(03)	0.4	0.511361(21)	0.348422(25)	0.511107	−18.0(0.4)	10
AP1	2007.10.24	0.0828(07)	0.6	0.511356(36)	0.348421(24)	0.511098	−18.1(0.7)	90
AP1	2007.10.25	0.0828(07)	0.9	0.511367(49)	0.348414(24)	0.511109	−17.9(0.9)	27
AP1	2008.01.09	0.0823(06)	0.8	0.511363(47)	0.348416(26)	0.511107	−18.0(0.9)	27
AP1	2008.11.06	0.0823(10)	1.2	0.511361(45)	0.348405(19)	0.511105	−18.0(0.8)	11
AP1	2008.11.07	0.0813(08)	1.0	0.511352(46)	0.348392(32)	0.511099	−18.1(0.9)	12
AP1	2009.05.03	0.0817(11)	1.3	0.511356(34)	0.348404(29)	0.511101	−18.1(0.7)	40
AP1	2010.10.05	0.0827(10)	1.2	0.511340(38)	0.348397(15)	0.511082	−18.4(0.8)	11
AP1	2010.10.06	0.0829(08)	1.0	0.511337(40)	0.348397(17)	0.511080	−18.5(0.8)	09
AP1	2010.10.09	0.0820(11)	1.4	0.511353(35)	0.348405(13)	0.511098	−18.1(0.7)	12
AP1	2010.10.10	0.0827(02)	0.2	0.511362(45)	0.348408(18)	0.511104	−18.0(0.9)	17
AP1	2010.10.22	0.0831(04)	0.5	0.511359(30)	0.348395(17)	0.511101	−18.1(0.6)	12
AP1	2010.12.26	0.0813(05)	0.7	0.511343(32)	0.348408(16)	0.511091	−18.3(0.6)	12
AP1	2010.12.27	0.0817(12)	1.5	0.511340(34)	0.348407(17)	0.511086	−18.4(0.6)	14
AP1	2010.12.28	0.0817(02)	1.5	0.511342(37)	0.348403(26)	0.511088	−18.3(0.7)	12
AP1	2010.12.29	0.0818(05)	0.7	0.511344(32)	0.348432(48)	0.511089	−18.3(0.6)	12
AP1	2010.12.30	0.0827(11)	1.4	0.511344(27)	0.348435(23)	0.511087	−18.3(0.5)	30
AP1	2011.02.17	0.0822(08)	1.0	0.511343(37)	0.348404(17)	0.511087	−18.3(0.7)	17
AP1	2012.04.19	0.0826(06)	0.7	0.511345(37)	0.348413(28)	0.511088	−18.3(0.7)	11
AP1	2012.09.10	0.0819(06)	0.8	0.511374(34)	0.348407(16)	0.511120	−17.7(0.7)	10
AP1	**Mean**	**0.0822(14)**	**1.6**	**0.511349(38)**	**0.348410(34)**	**0.511094(39)**	**−18.2(0.8)**	**396**
Durango Chew	2011.11.05	0.0882(09)	1.0	0.512500(33)	0.348409(33)	0.512482	−2.27(0.64)	8
Durango Chew	2011.11.06	0.0883(20)	2.3	0.512495(50)	0.348405(32)	0.512477	−2.36(0.97)	32
Durango Chew	2011.11.07	0.0882(17)	2.0	0.512490(34)	0.348407(20)	0.512472	−2.46(0.66)	55
Durango Chew	2012.09.10	0.0882(23)	2.6	0.512500(46)	0.348410(24)	0.512482	−2.27(0.90)	22
Durango Chew	2012.09.11	0.0890(13)	1.5	0.512496(34)	0.348402(21)	0.512478	−2.35(0.67)	24
Durango Chew	2012.09.12	0.0893(05)	0.6	0.512474(60)	0.348391(22)	0.512456	−2.77(1.16)	20
Durango Chew	2012.09.13	0.0888(30)	3.4	0.512467(59)	0.348401(52)	0.512449	−2.91(1.16)	13
Durango Chew	2012.09.16	0.0882(15)	1.7	0.512495(28)	0.348412(27)	0.512477	−2.36(0.55)	17
Durango Chew	**Mean**	**0.0885(19)**	**2.2**	**0.512490(46)**	**0.348405(29)**	**0.512472(46)**	**−2.45(0.90)**	**191**
Durango Fisher	2013.08.01	0.0765(12)	1.5	0.512477(39)	0.348410(26)	0.512462	−2.66(0.75)	31
Durango Griffin	2013.08.01	0.0840(17)	2.1	0.512491(28)	0.348416(19)	0.512474	−2.43(0.55)	30
Durango Hou	2013.08.01	0.0846(06)	0.7	0.512484(20)	0.348414(13)	0.512467	−2.56(0.39)	30
Durango Chew	2013.08.01	0.0905(20)	2.2	0.512497(25)	0.348419(15)	0.512478	−2.34(0.48)	30
MAD	2011.11.07	0.0805(06)	0.7	0.511321(33)	0.348405(22)	0.511066	−18.5(0.6)	60
MAD	2012.09.10	0.0814(13)	1.6	0.511333(67)	0.348404(25)	0.511075	−18.3(1.3)	23
MAD	2012.09.11	0.0813(17)	2.1	0.511309(59)	0.348390(22)	0.511051	−18.8(1.2)	24
MAD	2012.09.12	0.0819(17)	2.1	0.511308(51)	0.348394(30)	0.511048	−18.9(1.0)	17
MAD	2012.09.13	0.0813(17)	2.1	0.511320(60)	0.348401(52)	0.511062	−18.6(1.2)	12
MAD	2012.09.16	0.0817(22)	2.7	0.511338(48)	0.348412(26)	0.511078	−18.3(0.9)	18
MAD	**Mean**	**0.0811(17)**	**2.2**	**0.511322(53)**	**0.348402(30)**	**0.511064(53)**	**−18.5(1.0)**	**154**
Otter Lake	2011.11.04	0.0824(26)	3.2	0.511940(39)	0.348416(31)	0.511447	−0.25(0.86)	64
Otter Lake	2011.11.05	0.0824(11)	1.3	0.511942(47)	0.348416(26)	0.511448	−0.23(0.88)	25
Otter Lake	2011.11.06	0.0819(13)	1.5	0.511940(44)	0.348416(42)	0.511450	−0.20(0.86)	30
Otter Lake	2011.11.07	0.0827(14)	1.7	0.511944(35)	0.348411(15)	0.511449	−0.22(0.78)	23
Otter Lake	2012.09.10	0.0834(20)	2.4	0.511946(62)	0.348411(20)	0.511447	−0.25(1.24)	23
Otter Lake	2012.09.11	0.0835(29)	3.5	0.511939(54)	0.348404(20)	0.511438	−0.42(0.99)	23
Otter Lake	2012.09.12	0.0824(11)	1.4	0.511940(38)	0.348402(24)	0.511446	−0.27(0.75)	20
Otter Lake	2012.09.13	0.0824(30)	3.6	0.511940(36)	0.348409(24)	0.511446	−0.27(0.52)	11
Otter Lake	2012.09.16	0.0830(14)	1.6	0.511950(27)	0.348412(20)	0.511453	−0.13(0.62)	17
Otter Lake	**Mean**	**0.0827(21)**	**2.5**	**0.511942(45)**	**0.348411(28)**	**0.511447(45)**	**−0.25(0.88)**	**236**
NW-1	2009.11.08	0.1013(09)	0.9	0.512119(34)	0.348387(20)	0.511348	+4.07(0.63)	20
NW-1	2010.10.09	0.1013(10)	0.9	0.512137(20)	0.348416(24)	0.511366	+4.42(0.33)	16
NW-1	2013.08.01	0.1000(12)	1.2	0.512095(31)	0.348412(19)	0.511333	+3.77(0.64)	19
NW-1	2013.08.02	0.1021(12)	1.2	0.512106(29)	0.348407(11)	0.511328	+3.68(0.53)	10
NW-1	**Mean**	**0.1010(18)**	**1.7**	**0.512114(43)**	**0.348404(31)**	**0.511345(40)**	**+4.01(0.78)**	**65**
UWA-1	2013.08.01	0.1168(33)	2.9	0.512295(24)	0.348417(23)	0.510712	+14.5(0.7)	18
UWA-1	2013.08.02	0.1195(25)	2.1	0.512291(25)	0.348422(26)	0.510672	+13.7(0.7)	10
UWA-1	2013.08.04	0.1214(28)	2.3	0.512308(52)	0.348409(34)	0.510662	+13.5(1.6)	24
UWA-1	2013.08.05	0.1211(30)	2.5	0.512314(66)	0.348407(50)	0.510673	+13.7(1.4)	21
UWA-1	**Mean**	**0.1199(48)**	**4.0**	**0.512304(51)**	**0.348412(37)**	**0.510679(74)**	**+13.9(1.5)**	**73**
Mud Tank	2014.01.15	0.1012(04)	0.4	0.512361(111)	0.348386(64)	0.512054	+0.25(2.15)	15
McClure Mountain	2014.01.15	0.0696(72)	10	0.512246(80)	0.348394(43)	0.512007	+0.86(1.62)	15
SDG	2014.01.15	0.0721(04)	0.5	0.510948(46)	0.348405(22)	0.510188	−7.41(0.90)	20

Bold data indicate the mean value of corresponding item for apatite reference materials.

(McDowell et al., 2005). It is a widely used and distributed apatite reference material, and is extensively used in apatite fission track dating, apatite (U–Th)/He dating and apatite electron microprobe analyses around the world. Its chemical composition is well established although some variations have been documented (Frei et al., 2005; Trotter and Eggins, 2006; Morishita et al., 2008). Recently, Chew et al. (2011, 2014) used it as a potential secondary reference material for LA-ICP-MS U–Th–Pb apatite dating. In this study, a reference age of 31 Ma is adopted to correct for radiogenic ingrowth of ^{143}Nd (Zhou, 2013).

To date, of the eleven apatite reference materials considered in this study, only Sr and Nd isotope compositions of AP1, AP2 and Durango apatite have been previously analyzed by solution and laser ablation

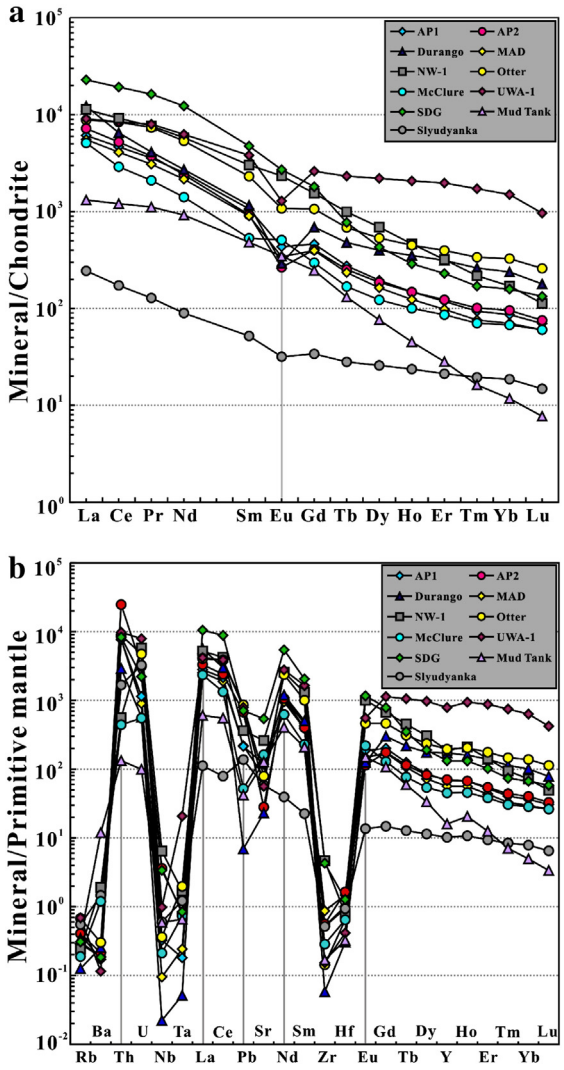

Fig. 1. Chondrite-normalized REE distribution patterns (a) and mantle-normalized patterns or "spidergrams" (b) of the apatite reference materials analyzed in this study. Normalization values for both primitive mantle and chondrite are from McDonough and Sun (1995).

techniques (Table 5). McFarlane and McCulloch (2008) obtained a mean $^{87}Sr/^{86}Sr$ ratio of 0.70629 ± 2 (2SD) for Durango apatite by TIMS, and a mean $^{87}Sr/^{86}Sr$ value of 0.70638 ± 13 (2SD, n = 8) by LA-MC-ICP-MS. Recently, Hou et al. (2013) obtained a mean $^{87}Sr/^{86}Sr$ ratio of 0.70629 ± 9 (2SD, n = 27) for Durango apatite by LA-MC-ICP-MS using an 80 μm laser spot size, and a TIMS mean $^{87}Sr/^{86}Sr$ ratio of 0.70634 ± 3 (2SD, n = 6).

Nd isotopic data for Durango apatite have been reported by four laboratories since 2006 using either solution-based or laser ablation techniques (Table 6). Foster and Vance (2006) first reported a mean $^{143}Nd/^{144}Nd$ ratio of 0.512483 ± 4 (2SD, n = 4) and a $^{147}Sm/^{144}Nd$ value of 0.0867 ± 1(2SD, n = 4) based on analysis of four separate aliquots by solution mode MC-ICP-MS. Subsequently, Fisher et al. (2011b) obtained a mean $^{143}Nd/^{144}Nd$ ratio of 0.512489 ± 12 (2SD, n = 8) and a $^{147}Sm/^{144}Nd$ ratio of 0.0751 ± 25 (2SD, n = 8) by solution mode MC-ICP-MS, with one outlier of 0.512459 ± 6 ($2\sigma_m$) excluded. Recently, Hou et al. (2013) presented a mean $^{143}Nd/^{144}Nd$ ratio of 0.512487 ± 13 (2SD, n = 6) and a $^{147}Sm/^{144}Nd$ ratio of 0.0865 ± 17 (2SD, n = 6) by ID-TIMS, and obtained $^{143}Nd/^{144}Nd$ and $^{147}Sm/^{144}Nd$ ratios of 0.512498 ± 25 (2SD, n = 25) and 0.0852 ± 10 (2SD, n = 25), respectively using LA-MC-ICP-MS. More recently, Kimura et al. (2013a) reported a mean $^{143}Nd/^{144}Nd$ ratio of 0.512490 ± 18 (2SD, n = 15) and a $^{147}Sm/^{144}Nd$ ratio of 0.0811 ± 21 (2SD, n = 15) by LA-MC-ICP-MS.

In this study we obtained four Durango apatite reference materials from four colleagues (D.M. Chew, C.M. Fisher, W.L. Griffin and K. J. Hou). The Durango_Chew apatite in this study is 3.0 cm × 1.5 cm × 1.0 cm while all others are small grains. Therefore, we conducted both solution and laser ablation analyses on the Durango_Chew apatite while we used the other three Durango apatite samples for laser ablation analyses only. The homogeneity of the four Durango apatite reference materials is discussed in the following section.

REE analyses indicate that Durango_Chew is LREE enriched with a moderate negative Eu anomaly (Fig. 1a). During a two-year period, LA-MC-ICP-MS analyses of Durango_Hou yielded $^{87}Sr/^{86}Sr$ ratios ranging from 0.70632 ± 14 (2SD, n = 55) to 0.70640 ± 13 (2SD, n = 16) with an average value of 0.70634 ± 14 (2SD, n = 156) (Table 2), which is consistent with the $^{87}Sr/^{86}Sr$ value of 0.706328 ± 23 (2SD, n = 13) from solution-based (TIMS and MC-ICP-MS) analyses of Durango _Chew (Fig. 3a). In contrast, the corresponding mean $^{84}Sr/^{86}Sr$ and $^{84}Sr/^{88}Sr$ of 0.0556 ± 10 (2SD, n = 156) and 0.00664 ± 12 (2SD, n = 156) of Durango_Hou (Table 2) are significantly lower than the published values of 0.0565 and 0.00675 because this sample was particularly susceptible to inaccurate isobaric interference corrections because of its low Sr and high HREE contents (Bizzarro et al., 2003; Ramos et al., 2004; Woodhead et al., 2005; McFarlane and McCulloch, 2008; Wu et al., 2010a; Yang et al., 2011a).

During a two-year period, LA-MC-ICP-MS analyses of Durango_Chew indicate that this reference material is relatively homogeneous in terms of its Nd isotopic composition. $^{143}Nd/^{144}Nd$ ratios range from 0.512467 ± 59 (2SD, n = 13) to 0.512500 ± 46 (2SD, n = 22) with an average value of 0.512490 ± 46 (2SD, n = 191). Meanwhile, the $^{147}Sm/^{144}Nd$ ratios varied from 0.0882 ± 23 (2SD, n = 22) to 0.0893 ± 5(2SD, n = 20) with an average value of 0.0885 ± 19 (2SD, n = 191) (Fig. 3b, Table 3). To assess accurately the variation in the LA-MC-ICP-MS Nd isotopic analyses, ten different chips produced during the crushing of a single large crystal of Durango Chew apatite were selected at random for solution mode MC-ICP-MS analyses. Our analyses yielded a mean $^{143}Nd/^{144}Nd$ of 0.512493 ± 21 (2SD, n = 11) (Table 3), which is in good agreement with published solution MC-ICP-MS or ID-TIMS Nd isotopic data (Foster and Vance, 2006; Fisher et al, 2011b; Hou et al., 2013, Table 6). The $^{147}Sm/^{144}Nd$ ratio of Durango_Chew apatite yielded a mean value of 0.0881 ± 11 (2SD, n = 9), which is somewhat higher than the published solution ICP-MS ratios of 0.0867, 0.0751 and 0.0865 (Foster and Vance, 2006; Fisher et al, 2011b; Hou et al., 2013, Table 6). The mean $^{145}Nd/^{144}Nd$ ratio of 0.348405 ± 29 (2SD, n = 191) is consistent with the recommended value of 0.348415 (Table 3). The corresponding $\varepsilon_{Nd(t)}$ value for Durango_Chew apatite is −2.40 ± 0.44 (2SD, n = 9), which is within uncertainty of the $\varepsilon_{Nd(t)}$ value of −2.45 ± 0.90 (2SD, n = 191) obtained by LA-MC-ICP-MS (Table 3, Fig. 3b).

3.3. MAD apatite

MAD (Madagascar apatite) is a large fragment of a blue gem quality apatite crystal from the 1st Mine Discovery in Madagascar. ID-TIMS analyses of four small crystal fragments of another crystal from the same mine yielded a weighted $^{206}Pb/^{238}U$ age of 485.2 ± 0.8 Ma after correction for common Pb (Thomson et al., 2012; Zhou, 2013). The crystal fragments analyzed in this study have Sr, Nd and Sm concentrations of ~1650, 1290 and 173 ppm and a reference age of ~485 Ma is used to calculate for ingrowth of radiogenic Nd (Table 1). REE analyses by LA-ICP-MS indicate that MAD apatite is LREE enriched, with a weak negative Eu anomaly similar to that of AP1 and AP2 apatite (Fig. 1a).

During a two-year period, LA-MC-ICP-MS analyses of MAD apatite yielded $^{87}Sr/^{86}Sr$ ratios that ranged from 0.71177 ± 9 (2SD, n = 26) to 0.71186 ± 14 (2SD, n = 20) with an average value of 0.71180 ± 11 (2SD, n = 112) (Table 2), which is consistent with the TIMS and

Table 4
Sr and Nd isotopic data of the apatite reference materials using solution method in this study.

Apatites	Sr [ppm]	$^{87}Sr/^{86}Sr$ ($\pm 2\sigma_m$)	Sm [ppm]	Nd [ppm]	$[^{147}Sm/^{144}Nd]_m$	$[^{143}Nd/^{144}Nd]_m$ ($\pm 2\sigma_m$)	$[^{143}Nd/^{144}Nd]_i$	$\varepsilon_{Nd(t)}$
AP1 (475 Ma)								
1*	2470	0.711390(12)	208	1513	0.0831	0.511381(07)	0.511122	−17.6
2*	2633	0.711365(12)	208	1521	0.0828	0.511344(08)	0.511086	−18.4
3*	2537	0.711376(19)	209	1523	0.0830	0.511348(08)	0.511090	−18.3
4*	2608	0.711394(14)	219	1580	0.0836	0.511369(07)	0.511109	−17.9
5*		0.711382(18)				0.511357(16)		
6		0.711358(18)	213	1570	0.0820	0.511341(09)	0.511086	−18.4
7		0.711382(21)	213	1571	0.0820	0.511341(09)	0.511086	−18.4
8		0.711355(21)	210	1551	0.0819	0.511345(08)	0.511090	−18.3
9a		0.711381(22)	216	1589	0.0822	0.511347(09)	0.511091	−18.3
9b**		0.711353(18)						
10		0.711354(13)	208	1526	0.0825	0.511356(07)	0.511100	−18.1
11		0.711345(15)	210	1548	0.0820	0.511348(08)	0.511093	−18.2
12a		0.711375(17)				0.511352(09)		
12b**		0.711359(18)						
Mean (±2SD)	**2562(147)**	**0.711370(31)**	**211(7)**	**1549(55)**	**0.0825(12)**	**0.511352(24)**	**0.511095**	**−18.2(0.5)**
AP2 (475 Ma)								
1*	643	0.726522(12)	192	1522	0.0762	0.511022(08)	0.510785	−24.2
2*	622	0.726543(21)	190	1500	0.0765	0.510984(09)	0.510746	−25.0
3*	646	0.726555(21)	178	1410	0.0762	0.510987(08)	0.510750	−24.9
4*		0.726592(20)				0.510982(24)		
5		0.726543(19)	178	1404	0.0764	0.511010(06)	0.510772	−24.5
6		0.726537(23)	177	1399	0.0764	0.511018(07)	0.510780	−24.3
7		0.726541(20)	183	1445	0.0764	0.511014(08)	0.510776	−24.4
8		0.726495(21)	181	1436	0.0763	0.511026(06)	0.510789	−24.2
9		0.726543(18)	177	1408	0.0761	0.511012(10)	0.510775	−24.4
10a		0.726555(21)	178	1405	0.0765	0.511013(08)	0.510775	−24.4
10b**		0.726527(18)						
11		0.726561(23)	181	1435	0.0764	0.511013(10)	0.510775	−24.4
12		0.726538(19)				0.511003(12)		
Mean (±2SD)	**637(26)**	**0.726542(45)**	**181(11)**	**1436(86)**	**0.0764(2)**	**0.511007(30)**	**0.510769**	**−24.5(0.5)**
Durango Chew (31 Ma)								
1a		0.706304(14)	238	1635	0.0882	0.512495(07)	0.512477	−2.36
1b**		0.706342(20)						
2		0.706327(17)	242	1648	0.0886	0.512501(11)	0.512483	−2.24
3a		0.706324(20)	243	1655	0.0887	0.512472(22)	0.512454	−2.82
3b**		0.706342(20)						
4		0.706312(15)	240	1640	0.0884	0.512481(09)	0.512464	−2.63
5		0.706337(24)	252	1731	0.0881	0.512492(08)	0.512474	−2.41
6		0.706336(16)	234	1602	0.0882	0.512508(08)	0.512490	−2.12
7		0.706332(15)	246	1702	0.0874	0.512504(07)	0.512486	−2.18
8		0.706331(19)	246	1690	0.0879	0.512496(10)	0.512479	−2.33
9		0.706330(13)				0.512497(08)	0.512497	
10		0.706319(16)				0.512493(07)	0.512493	
11		0.706336(16)	245	1698	0.0871	0.512484(12)	0.512496	−2.40
Mean (±2SD)		**0.706328(23)**	**243(11)**	**1667(82)**	**0.0881(11)**	**0.512493(21)**	**0.512475**	**−2.40(0.44)**
MAD (485 Ma)								
1a		0.711778(18)	181	1337	0.0817	0.511343(09)	0.511083	−18.2
1b**		0.711785(18)						
2		0.711793(20)	180	1330	0.0817	0.511357(09)	0.511098	−17.9
3a		0.711796(27)	183	1348	0.0823	0.511350(11)	0.511089	−18.1
3b**		0.711814(18)						
4a		0.711787(27)	172	1269	0.0817	0.511353(08)	0.511093	−18.0
4b**		0.711818(20)						
5		0.711791(25)	179	1325	0.0816	0.511358(08)	0.511098	−17.9
6		0.711798(20)				0.511349(08)		
7		0.711814(16)				0.511339(07)		
8		0.711800(17)				0.511337(09)		
Mean (±2SD)		**0.711798(26)**	**179(9)**	**1322(61)**	**0.0818(5)**	**0.511348(16)**	**0.511088**	**−18.1(0.3)**
Otter Lake (913 Ma)								
1		0.704190(26)	514	3781	0.0821	0.511935(09)	0.511444	−0.32
2a		0.704185(13)	485	3550	0.0826	0.511946(08)	0.511451	−0.17
2b**		0.704204(18)						
3		0.704197(24)	499	3650	0.0826	0.511941(08)	0.511446	−0.27
4		0.704172(15)	485	3548	0.0826	0.511936(10)	0.511441	−0.37
5a		0.704160(22)	488	3590	0.0823	0.511945(09)	0.511452	−0.16
5b**		0.704184(20)						
6a		0.704197(14)				0.511942(08)		
6b**		0.704200(18)						
7		0.704190(11)				0.511935(09)		
Mean (±2SD)		**0.704188(27)**	**494(25)**	**3624(195)**	**0.0824(4)**	**0.511940(09)**	**0.511446**	**−0.27(0.18)**

Table 4 *(continued)*

Apatites	Sr [ppm]	$^{87}Sr/^{86}Sr$ ($\pm 2\sigma_m$)	Sm [ppm]	Nd [ppm]	$[^{147}Sm/^{144}Nd]_m$	$[^{143}Nd/^{144}Nd]_m$ ($\pm 2\sigma_m$)	$[^{143}Nd/^{144}Nd]_i$	$\varepsilon_{Nd(t)}$
NW-1 (1160 Ma)								
1		0.702507(19)	611	3640	0.1015	0.512112(09)	0.511339	+3.90
2a		0.702492(17)	608	3628	0.1012	0.512100(10)	0.511329	+3.70
2b**		0.702509(20)						
3		0.702497(19)	615	3648	0.1018	0.512111(10)	0.511335	+3.82
4a		0.702505(19)	590	3514	0.1014	0.512105(10)	0.511332	+3.76
4b**		0.702509(20)						
5		0.702487(12)	604	3613	0.1011	0.512103(09)	0.511333	+3.78
6a		0.702495(10)				0.512099(07)		
6b**		0.702515(20)						
7		0.702507(14)	650	3875	0.1013	0.512108(09)	0.511337	+3.84
8		0.702515(14)	625	3746	0.1008	0.512097(09)	0.511330	+3.71
Mean (±2SD)		**0.702504(19)**	**614(38)**	**3666(229)**	**0.1013(6)**	**0.512104(11)**	**0.511333**	**+3.77(0.14)**
Slyudyanka (460 Ma)								
1a		0.707690(18)						
1b**		0.707680(20)						
2a		0.707680(21)						
2b**		0.707683(20)						
3		0.707688(19)						
4		0.707667(12)						
5		0.707704(16)						
6a		0.707669(15)						
6b**		0.707666(32)						
7		0.707695(20)						
8		0.707693(19)						
Mean (±2SD)		**0.707683(25)**						
UWA-1 (2058 Ma)								
1		0.704744(17)	738	3722	0.1198	0.512294(08)	0.510671	+13.7
2		0.704751(23)	758	3850	0.1191	0.512285(09)	0.510672	+13.7
3		0.704742(14)	762	3903	0.1181	0.512284(10)	0.510684	+13.9
4		0.704749(21)	768	3913	0.1187	0.512279(08)	0.510671	+13.7
5		0.704755(16)	787	4011	0.1187	0.512289(08)	0.510681	+13.9
6		0.704760(30)	762	3915	0.1177	0.512287(07)	0.510691	+14.1
7		0.704736(19)				0.512284(11)		
Mean (±2SD)		**0.704748(17)**	**763(32)**	**3886(191)**	**0.1187(14)**	**0.512286(09)**	**0.510678**	**+13.8(0.3)**
Mud Tank (460 Ma)								
1		0.703031(16)	92	552	0.1004	0.512383(08)	0.512079	+0.73
2		0.702996(14)	97	592	0.0991	0.512375(08)	0.512075	+0.73
3		0.703010(13)	94	561	0.1009	0.512388(07)	0.512082	+0.73
4		0.703013(12)	94	562	0.1009	0.512391(10)	0.512085	+0.73
5		0.703004(15)	93	558	0.1010	0.512388(08)	0.512082	+0.73
Mean (±2SD)		**0.703011(26)**	**94(4)**	**565(31)**	**0.1005(16)**	**0.512385(13)**	**0.512080**	**+0.76(0.16)**
McClure Mountain (523.5 Ma)								
1		0.703705(33)	98	825	0.0715	0.512289(07)	0.512044	+1.58
2		0.703687(14)	98	825	0.0715	0.512289(07)	0.512039	+1.47
3		0.703684(13)	98	835	0.0708	0.512289(07)	0.512032	+1.34
4		0.703694(15)	98	835	0.0708	0.512289(07)	0.512037	+1.44
5		0.703690(15)	102	861	0.0716	0.512289(07)	0.512038	+1.47
Mean (±2SD)		**0.703692(16)**	**99(4)**	**836(29)**	**0.0712(8)**	**0.512282(11)**	**0.512038**	**+1.46(0.17)**
SDG (1602 Ma)								
1		0.703012(14)	989	8282	0.0722	0.510907(05)	0.510146	−8.23
2		0.703001(14)	974	8136	0.0723	0.510921(09)	0.510159	−7.98
3		0.703010(13)	973	8137	0.0723	0.510917(10)	0.510156	−8.05
4		0.703002(24)	994	8466	0.0710	0.510924(06)	0.510176	−7.64
5		0.702997(16)	969	8176	0.0717	0.510923(10)	0.510168	−7.80
Mean (±2SD)		**0.703004(13)**	**980(22)**	**8239(280)**	**0.0719(11)**	**0.510918(14)**	**0.510161**	**−7.94(0.46)**

*Measured by IsoProbe-T TIMS, **measured by Triton Plus TIMS and others measured by Neptune MC-ICP-MS.
a and b means the Sr fraction after standard cation and Sr-Specific resin is divided to two aliquots, in which a aliquot's Sr isotopic ratio measured by Neptune MC-ICP-MS and b aliquot's Sr isotopic ratio measured by Triton Plus TIMS.
Measured Sr and Nd isotopic ratios are normalized to the following recommended values: NBS 987 $^{87}Sr/^{86}Sr = 0.710250$ (Thirlwall, 1991) and JNdi-1 $^{143}Nd/^{144}Nd = 0.512110$, equivalent to La Jolla $^{143}Nd/^{144}Nd$ Value of 0.51185.
Initial isotope ratios calculated for the standard apatite recommended age value, which are the numbers in parentheses after standard apatite name in the first column.
Calculated using ^{147}Sm decay constant of 6.54×10^{-12} a^{-1} (Lugmair and Marti, 1978); $[^{143}Nd/^{144}Nd]_{CHUR} = 0.512638$ (Goldstein et al., 1984) and $[^{147}Sm/^{144}Nd]_{CHUR} = 0.1967$ (Jacobsen and Wasserburg, 1980).
Bold data indicate the mean value of corresponding item for apatite reference materials.

MC-ICP-MS average value of 0.711798 ± 26 (2SD, n = 8) (Table 4, Fig. 3c). The $^{87}Sr/^{86}Sr$ data in different analytical sessions are consistent within analytical uncertainty. Furthermore, the corresponding mean $^{84}Sr/^{86}Sr$ and $^{84}Sr/^{88}Sr$ ratios of 0.0565 ± 5 (2SD, n = 112) and 0.00675 ± 6 (2SD, n = 112) agree well with published values (Bizzarro et al., 2003; Ramos et al., 2004; Woodhead et al., 2005; Yang et al., 2011a) (Table 2).

$^{143}Nd/^{144}Nd$ data for MAD apatite ranged from 0.511308 ± 51 (2SD, n = 17) to 0.511338 ± 48 (2SD, n = 18) with an average value of 0.511322 ± 53 (2SD, n = 154). $^{147}Sm/^{144}Nd$ ratios varied

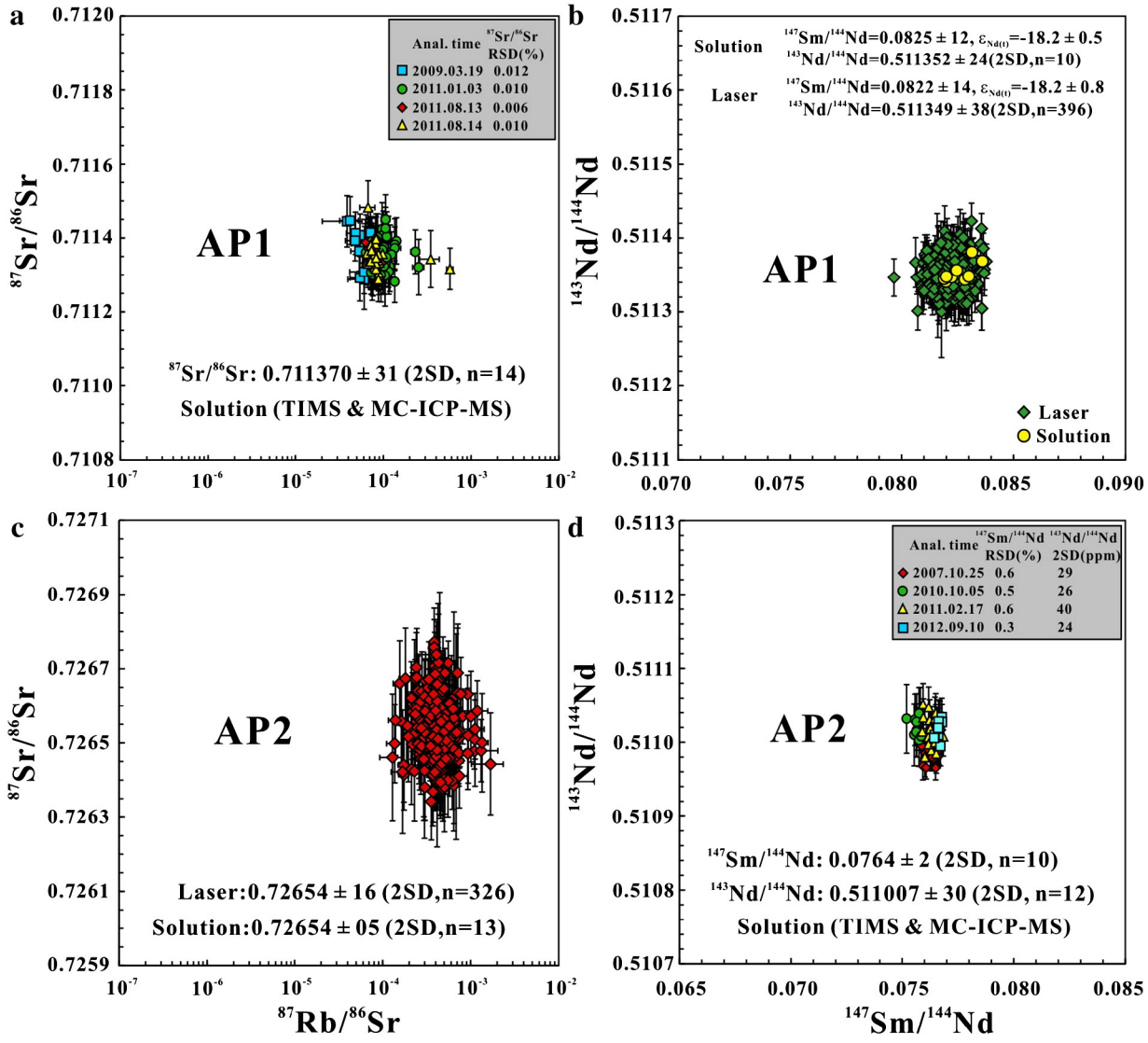

Fig. 2. Measured $^{87}Sr/^{86}Sr$, $^{147}Sm/^{144}Nd$ and $^{143}Nd/^{144}Nd$ isotopic ratios determined by LA-MC-ICP-MS and compared to solution data for apatite crystals AP1 (a, b) and AP2 (c, d). Error bars for individual analyses are 2S.E. (2 standard in-run errors). Relative standard deviation (RSD) is used to evaluate the range of variation in $^{147}Sm/^{144}Nd$. We selected AP1 as Sr isotope reference material and AP2 as a Nd isotope external reference material for subsequent analytical sessions.

from 0.0805 ± 6 (2SD, n = 60) to 0.0819 ± 17 (2SD, n = 17) with an average value of 0.0811 ± 17 (2SD, n = 154). The $^{145}Nd/^{144}Nd$ ratio of 0.348402 ± 30 (2SD, n = 154) is consistent with the published value of 0.348415 (Wasserburg et al., 1981; Liu et al., 2012) (Table 3). In order to assess the accuracy of the LA-MC-ICP-MS results, eight different chips derived from crushing a larger fragment of a crystal of MAD apatite were selected at random for solution mode MC-ICP-MS analyses (Table 4), yielding a mean $^{143}Nd/^{144}Nd$ ratio of 0.511348 ± 16 (2SD, n = 8) (Fig. 3d) and a $^{147}Sm/^{144}Nd$ ratio of 0.0818 ± 5 (2SD, n = 5). These solution-based data are within analytical uncertainty of the LA-MC-ICP-MS values. The corresponding $\varepsilon_{Nd(t)}$ value for MAD apatite is −18.1 ± 0.3 (2SD, n = 5) for the solution-based analyses which is with analytical uncertainty of the LA-MC-ICP-MS value of −18.5 ± 1.0 (2SD, n = 154) (Table 4, Fig. 3d).

3.4. Otter Lake apatite

The Otter Lake area, Québec, Canada, is located north of the Bancroft domain within the Grenville Province. The rocks of the Otter Lake area comprise marbles, gneisses, amphibolites, and skarns that underwent upper-amphibolite-facies metamorphism at temperatures and pressures of 650 to 700 °C and 6.5–7 kbar in connection with the Elzevirian and Ottowan phases of the Grenville orogeny (Kretz et al., 1999; Barfod et al., 2005). Pb stepwise leaching analyses and bulk dissolutions of a single apatite crystal in calcite from Yates Mine, Otter Lake yield a $^{207}Pb/^{204}Pb$–$^{206}Pb/^{204}Pb$ isochron age of 913 ± 7 Ma, which is the reference age adopted in this study (Barfod et al., 2005; Chew et al., 2011). The Sr, Sm and Nd concentration estimates by LA-ICP-MS are 1668, 445 and 3205 ppm respectively (Table 1). REE analysis indicates that Otter Lake is LREE enriched with a slight negative Eu anomaly (Fig. 1a).

During a two-year period, LA-MC-ICP-MS analyses of Otter Lake apatite yielded $^{87}Sr/^{86}Sr$ ratios that ranged from 0.70419 ± 5 (2SD, n = 8) to 0.70424 ± 15 (2SD, n = 9) with an average value of 0.70421 ± 12 (2SD, n = 117) (Table 2), which is consistent with the TIMS and solution MC-ICP-MS average value of 0.704188 ± 27 (2SD, n = 7) (Table 4, Fig. 3e). The $^{87}Sr/^{86}Sr$ data from different analytical sessions are consistent within analytical uncertainty. The mean $^{84}Sr/^{86}Sr$ and $^{84}Sr/^{88}Sr$ ratios of 0.0566 ± 10 (2SD, n = 117) and 0.00676 ± 11 (2SD, n = 117) agree well with the recommended values of 0.0565 and 0.00675 (Bizzarro et al., 2003; Ramos et al., 2004; Woodhead et al., 2005; Yang et al., 2011a) (Table 2).

$^{143}Nd/^{144}Nd$ data of Otter Lake apatite ranged from 0.511940 ± 44 (2SD, n = 30) to 0.511950 ± 27 (2SD, n = 17) with an average value of 0.511942 ± 45 (2SD, n = 236), while the $^{147}Sm/^{144}Nd$ ratios ranged

Table 5
Compilations of Sr concentration and isotopic composition of the apatite reference materials.

Apatites	Sr [ppm] (±2SD)	$^{87}Sr/^{86}Sr$ (±2SD)	Methods	References
AP1	2582(23)	0.71137(07)	LA-MC-ICP-MS	Yang et al., 2009b
		0.71138(02)	Sol.-MC-ICP-MS	Yang et al., 2009b
		0.71136(09)	LA-MC-ICP-MS	Hou et al., 2013
	2506	0.71136(08)	LA-MC-ICP-MS	This study
	2562(147)	0.71137(03)	Solution method	This study
AP2	596(5)	0.72652(10)	LA-MC-ICP-MS	Yang et al., 2009b
		0.72655(02)	Sol.-MC-ICP-MS	Yang et al., 2009b
	591	0.72654(16)	LA-MC-ICP-MS	This study
	637(26)	0.72654(05)	Solution method	This study
Durango	475(11)	0.70638(13)	LA-MC-ICP-MS	McFarlane and McCulloch, 2008
		0.70629(02)	TIMS	McFarlane and McCulloch, 2008
		0.70629(09)	LA-MC-ICP-MS	Hou et al., 2013
	483	0.70634(03)	TIMS	Hou et al., 2013
	475(12)		LA-ICP-MS	Simonetti et al., 2008
	480(14)		Sol. ICP-MS	Simonetti et al., 2008
	462		LA-ICP-MS	Trotter and Eggins, 2006
	475(11)		Sol. ICP-MS	Trotter and Eggins, 2006
		0.70633(01)	TIMS	Horstwood et al., 2008
	486	0.70634(14)	LA-MC-ICP-MS	This study
		0.70633(02)	Solution method	This study
MAD		0.71180(11)	LA-MC-ICP-MS	This study
	1650	0.71180(03)	Solution method	This study
Otter Lake		0.70421(12)	LA-MC-ICP-MS	This study
	1668	0.70419(03)	Solution method	This study
NW-1		0.70248(08)	LA-MC-ICP-MS	This study
	5512	0.70250(02)	Solution method	This study
Slyudyanka	1231	0.70769(15)	LA-MC-ICP-MS	This study
		0.70768(03)	Solution method	This study
UWA-1		0.70475(02)	Solution method	This study
Mud Tank	2681	0.70302(08)	LA-MC-ICP-MS	This study
		0.70301(03)	Solution method	This study
McClure Mountain	3422	0.70371(07)	LA-MC-ICP-MS	This study
		0.70369(02)	Solution method	This study
SDG	11368	0.70298(16)	LA-MC-ICP-MS	This study
		0.70300(01)	Solution method	This study

from 0.0819 ± 13 (2SD, n = 30) to 0.0835 ± 29 (2SD, n = 23) with an average value of 0.0827 ± 21 (2SD, n = 236). The mean $^{145}Nd/^{144}Nd$ ratio of 0.348411 ± 28 (2SD, n = 236) is consistent with the published value of 0.348415 (Wasserburg et al., 1981; Liu et al., 2012) (Table 3). In order to assess the accuracy of the LA-MC-ICP-MS results, seven different chips derived from crushing a crystal of Otter Lake apatite were selected at random for solution mode MC-ICP-MS (Table 4), yielding a mean $^{143}Nd/^{144}Nd$ ratio of 0.511940 ± 10 (2SD, n = 7) (Fig. 3f) and a $^{147}Sm/^{144}Nd$ ratio of 0.0824 ± 4 (2SD, n = 5). These data are in very good agreement with the LA-ICP-MS results. The corresponding $\varepsilon_{Nd(t)}$ value for Otter Lake apatite is −0.27 ± 0.18 (2SD, n = 5), which is very similar to the LA-MC-ICP-MS value of −0.25 ± 0.88 (2SD, n = 236) (Table 4, Fig. 3f). The close agreement between the solution-based and LA-MC-ICP-MS analyses and the homogeneity in terms of its Sr and Sm–Nd isotopic compositions suggests that Otter Lake apatite is a promising reference material for *in situ* Sr or Nd analyses.

3.5. NW-1 apatite

NW-1 apatite was extracted from a carbonatite collected from the Prairie Lake alkaline carbonatite complex in Ontario, Canada, where the PRAP apatite reference material was collected (Sano et al., 1999; Wu et al., 2010a,b,c; Li et al., 2012; Zhou, 2013). There have been many geochronological investigations conducted on this complex over the years. As noted by Li et al. (2012), the best estimate for the U–Th–Pb age of NW-1 apatite is 1160 ± 5 Ma, which is the reference age adopted in this study. The Sr, Sm and Nd concentration estimates by LA-ICP-MS are 5512, 582 and 3468 ppm respectively (Table 1). NW-1 is LREE enriched and is unique among the reference apatite materials examined in this study in that it does not exhibit an Eu anomaly (Fig. 2a).

During the course of five LA-MC-ICP-MS sessions, the $^{87}Sr/^{86}Sr$ ratios of NW-1 apatite varied from 0.70246 ± 7 (2SD, n = 19) to 0.70249 ± 9 (2SD, n = 20) with an average value of 0.70248 ± 8 (2SD, n = 87) (Table 2), which is consistent with the TIMS and solution MC-ICP-MS average value of 0.702504 ± 19 (2SD, n = 11) (Table 4, Fig. 4a). The $^{87}Sr/^{86}Sr$ data from different analytical sessions are consistent with each other within analytical uncertainty. The mean $^{84}Sr/^{86}Sr$ and $^{84}Sr/^{88}Sr$ ratios of 0.0564 ± 4 (2SD, n = 87) and 0.00674 ± 4 (2SD, n = 87), respectively, agree well with the recommended values of 0.0565 and 0.00675 (Bizzarro et al., 2003; Ramos et al., 2004; Woodhead et al., 2005; Yang et al., 2011c, 2012) (Table 2).

$^{143}Nd/^{144}Nd$ ratios of NW-1 apatite varied from 0.512095 ± 31 (2SD, n = 19) to 0.512137 ± 10 (2SD, n = 16) over the course of four analytical sessions, while the $^{147}Sm/^{144}Nd$ varied from 0.1000 ± 12 (2SD, n = 19) to 0.1013 ± 10 (2SD, n = 16). The mean $^{145}Nd/^{144}Nd$ ratio of 0.348404 ± 31 (2SD, n = 65) is consistent with published values (Table 3). Additionally, eight aliquots derived from crushing a single large crystal of NW-1 apatite were selected at random for solution analyses, yielding a mean $^{143}Nd/^{144}Nd$ ratio of 0.512104 ± 11 (2SD, n = 8) (Table 4, Fig. 4b) and a mean $^{147}Sm/^{144}Nd$ value of 0.1013 ± 6 (2SD, n = 7). The corresponding $\varepsilon_{Nd(t)}$ value for NW-1 apatite is + 3.77 ± 0.14 (2SD, n = 7), which is within uncertainty of LA-MC-ICP-MS value of + 4.01 ± 0.78 (2SD, n = 65) (Table 3, Fig. 4b). There is close agreement between the solution-based and LA-MC-ICP-MS analyses, while NW-1 apatite appears relatively homogenous in terms of its Sr and Sm–Nd isotopic compositions and hence could make a promising reference material for *in situ* Sr or Nd analyses.

Table 6
Compilations of Sm, Nd concentration, Sm–Nd isotopic data and corresponding initial epsilon Nd of the apatite reference materials.

Apatites	Sm (±2SD) [ppm]	Nd (±2SD) [ppm]	$[^{147}Sm/^{144}Nd]_m$ (±2SD)	$[^{143}Nd/^{144}Nd]_m$ (±2SD)	$[^{143}Nd/^{144}Nd]_i$	$\varepsilon_{Nd(t)}$ (±2SD)	Methods	References
AP1	206(5)	1581(43)	0.0866(05)	0.511342(31)	0.511073	−18.6(0.6)	LA-MC-ICP-MS	Yang et al., 2008
(475 Ma)				0.511334(25)			Sol.-MC-ICP-MS	Yang et al., 2008
			0.0867(10)	0.511360(25)	0.511090	−18.3(0.5)	LA-MC-ICP-MS	Hou et al., 2013
	205	1501	0.0822(14)	0.511349(38)	0.511094	−18.2(0.8)	LA-MC-ICP-MS	This study
	211(7)	1549(55)	0.0825(12)	0.511352(24)	0.511095	−18.2(0.5)	Solution method	This study
AP2	180(4)	1495(34)	0.0794(13)	0.510977(39)	0.510730	−25.3(0.7)	LA-MC-ICP-MS	Yang et al., 2008
(475 Ma)				0.510985(08)			Sol.-MC-ICP-MS	Yang et al., 2008
	178	1435	0.0761(11)	0.511008(42)	0.510771	−24.5(0.8)	LA-MC-ICP-MS	This study
	181(11)	1436(86)	0.0764(02)	0.511007(30)	0.510769	−24.5(0.5)	Solution method	This study
Durango	229(47)	1598(325)	0.0867(07)	0.512483(04)	0.512465	−2.59(0.08)	Sol.-MC-ICP-MS	Foster and Vance, 2006
(31 Ma)								
			0.0752(10)	0.512470(32)	0.512455	−2.80(0.62)	LA-MC-ICP-MS	Foster and Vance, 2006
			0.0871(10)	0.512466(13)	0.512448	−2.92(0.25)	LA-MC-ICP-MS	Foster and Vance, 2006
	127(3.3)	1040(29)	0.0763(14)	0.512449(10)	0.512434	−3.21(0.20)	LA-MC-ICP-MS	McFarlane and McCulloch, 2008
			0.0765(05)	0.512469(16)	0.512453	−2.82(0.31)	LA-MC-ICP-MS	McFarlane and McCulloch, 2008
			0.0751(25)	0.512489(12)	0.512474	−2.43(0.23)	Sol.-MC-ICP-MS	Fisher et al., 2011b
			0.0785(58)	0.512463(48)	0.512447	−2.95(0.94)	LA-MC-ICP-MS	Fisher et al., 2011b
			0.0852(10)	0.512498(25)	0.512481	−2.29(0.49)	LA-MC-ICP-MS	Hou et al., 2013
	224(5)	1568(24)	0.0865(17)	0.512487(13)	0.512469	−2.51(0.25)	TIMS	Hou et al., 2013
			0.0811(21)	0.512490(18)	0.512474	−2.43(0.35)	LA-MC-ICP-MS	Kimura et al., 2013a
			0.0885(19)	0.512490(46)	0.512472	−2.45(0.90)	LA-MC-ICP-MS	This study
	243(11)	1667(82)	0.0881(11)	0.512493(21)	0.512475	−2.40(0.44)	Sol.-MC-ICP-MS	This study
MAD			0.0811(17)	0.511322(53)	0.511064	−18.5(1.0)	LA-MC-ICP-MS	This study
(485 Ma)	182(9)	1322(61)	0.0818(05)	0.511348(16)	0.511088	−18.1(0.3)	Sol.-MC-ICP-MS	This study
Otter Lake			0.0827(21)	0.511942(45)	0.511447	−0.25(0.88)	LA-MC-ICP-MS	This study
(913 Ma)	494(25)	3624(195)	0.0824(04)	0.511940(09)	0.511446	−0.27(0.18)	Sol.-MC-ICP-MS	This study
NW-1			0.1010(18)	0.512114(43)	0.511345	+4.01(0.78)	LA-MC-ICP-MS	This study
(1160 Ma)	614(38)	3666(109)	0.1013(06)	0.512104(11)	0.511333	+3.77(0.14)	Sol.-MC-ICP-MS	This study
UWA-1			0.1199(48)	0.512304(51)	0.510679	+13.9(1.5)	LA-MC-ICP-MS	This study
(2058 Ma)	763(32)	3886(191)	0.1187(14)	0.512286(09)	0.510678	+13.8(0.3)	Sol.-MC-ICP-MS	This study
Mud Tank			0.1012(04)	0.512361(111)	0.512054	+0.25(2.15)	LA-MC-ICP-MS	This study
(460 Ma)	94(4)	565(31)	0.1005(16)	0.512385(13)	0.512080	+0.76(0.16)	Sol.-MC-ICP-MS	This study
McClure Mountain			0.0696(72)	0.512246(80)	0.512007	+0.86(1.62)	LA-MC-ICP-MS	This study
(523.5 Ma)	99(4)	836(29)	0.0712(08)	0.512282(11)	0.512038	+1.46(0.17)	Sol.-MC-ICP-MS	This study
SDG			0.0721(04)	0.510948(46)	0.510188	−7.41(0.90)	LA-MC-ICP-MS	This study
(1602 Ma)	980(22)	8239(280)	0.0719(11)	0.510918(14)	0.510161	−7.94(0.46)	Sol.-MC-ICP-MS	This study

3.6. Slyudyanka apatite

The Slyudyanka complex is a granulite-facies supracrustal sequence that crops out on the southwest coast of Lake Baikal. The Slyudyanka complex is dominated by metamorphosed siliceous–carbonate phosphorites, which are composed of apatite (from 1–2 to 60 wt.%), quartz, diopside, calcite, forsterite and dolomite with minor retrograde tremolite (Reznitskii et al., 1998, 1999, 2000).

The Slyudyanka apatite investigated in this study (3.0 cm × 2.0 cm × 1.0 cm) was also supplied by D.M. Chew. The Sr, Sm and Nd concentration estimates by LA-ICP-MS are 1231, 10 and 53 ppm respectively (Dempster et al., 2003). Slyudyanka is LREE enriched with a slight negative Eu anomaly (Fig. 1a). Given its low REE contents, only Sr isotopic measurements were undertaken in this study (Fig. 4c). The $^{87}Sr/^{86}Sr$ data ranged from 0.70766 ± 13 (2SD, n = 20) to 0.70773 ± 21 (2SD, n = 13) in seven analytical sessions spread over a two-year period with an average value of 0.70769 ± 15 (2SD, n = 110). The mean $^{84}Sr/^{86}Sr$ and $^{84}Sr/^{88}Sr$ ratios of 0.0565 ± 7 (2SD, n = 110) and 0.00675 ± 9 (2SD, n = 110) agree well with the published values of 0.0565 and 0.00675 (Bizzarro et al., 2003; Ramos et al., 2004; Woodhead et al., 2005; Yang et al., 2011a) (Table 2). Additionally, eight different chips produced during the crushing of a single large crystal of Slyudyanka apatite were selected at random for analysis by TIMS and solution MC-ICP-MS. These analyses yielded a mean $^{87}Sr/^{86}Sr$ value of 0.707683 ± 25 (2SD, n = 11) (Table 4, Fig. 4c), which agrees well with the data obtained using LA-MC-ICP-MS. The Slyudyanka apatite appears to be a very promising candidate reference material for *in situ* apatite Sr isotopic measurements.

3.7. UWA-1 apatite

UWA-1 is a fluorapatite from Bancroft, Ontario that is widely used as an apatite U–Pb age reference material. It is also used as an apatite O isotope reference material in many SIMS laboratories. Its $^{206}Pb/^{238}U$ and $^{207}Pb/^{206}Pb$ ages are 2058 Ma and 2071 Ma respectively, and the $^{206}Pb/^{238}U$ age of 2058 Ma is the reference age adopted in this study (Zhou et al., 2007; Allen Kennedy, personal communication). The UWA-1 apatite investigated in this study was provided by John Valley. The Sr, Sm and Nd concentration estimates by LA-ICP-MS are 1186, 731 and 3747 ppm respectively. Though LREE enriched like the other samples, the REE pattern of UWA-1 is nevertheless distinct, showing less extreme LREE enrichment and the highest HREE levels of all of other apatite reference materials (Fig. 1a). For solution MC-ICP-MS Sr isotopic analyses, seven separate fragments of UWA-1 apatite were dissolved and separated using conventional ion chromatography methods. The Sr isotopic results obtained by MC-ICP-MS are listed in Table 4 and yield an average $^{87}Sr/^{86}Sr$ value of 0.704748 ± 17 (2SD, n = 7). UWA-1 apatite is not suitable for *in situ* Sr isotopic analyses despite its relative high Sr content (1186 ppm), because its high Er/Sr and Yb/Sr ratios are particularly susceptible to inaccurate isobaric interference corrections (Wu et al., 2010a). Four analytical sessions indicate that this material is relatively inhomogeneous in terms of its Sm–Nd isotopic

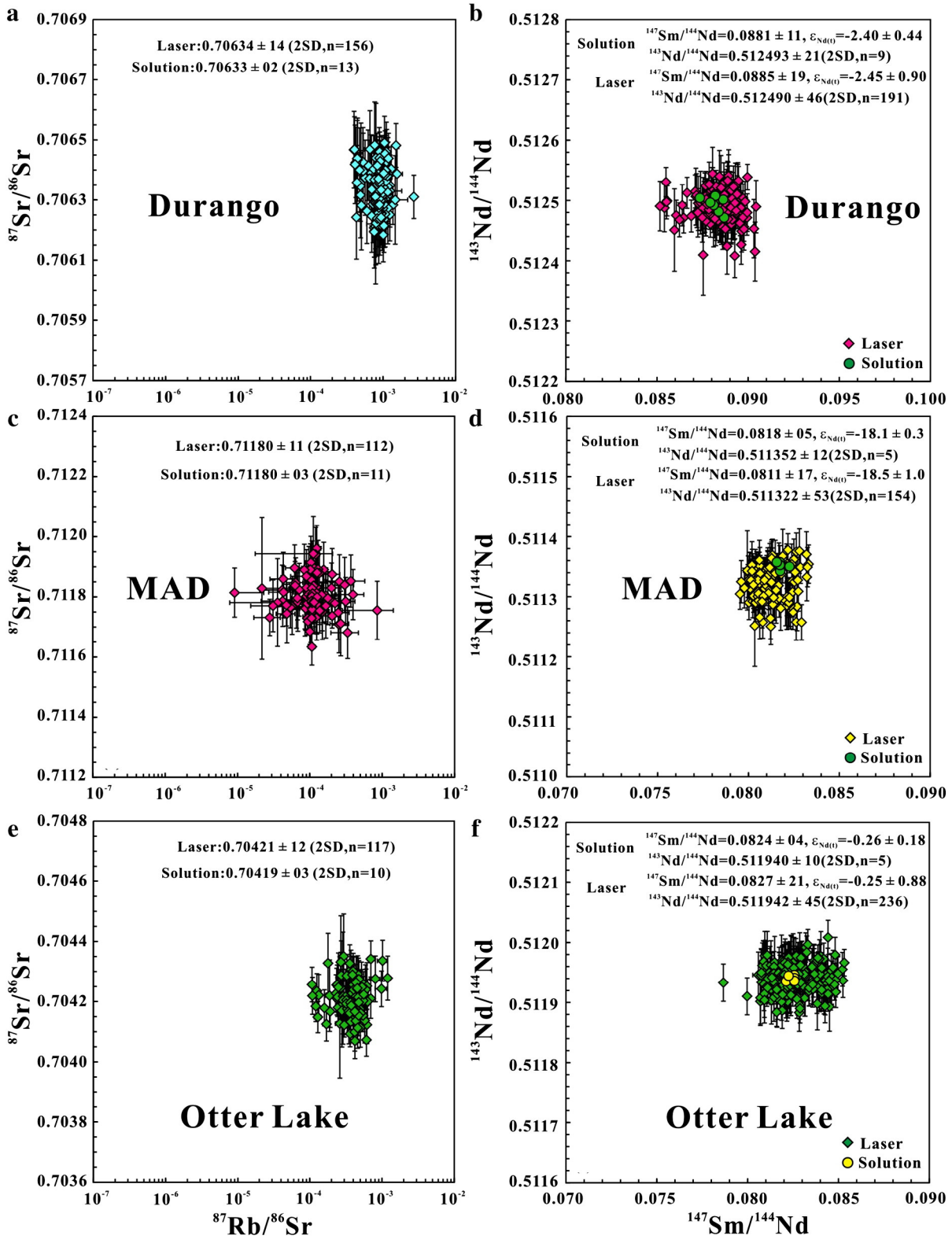

Fig. 3. Summary of measured Sr and Sm–Nd isotopic data for Durango (a, b), MAD (c, d) and Otter Lake (e, f) apatites analyzed by LA-MC-ICP-MS in different analytical sessions and compared to solution-based data. Compared to solution analyses, the laser analyses exhibit more scatter and larger uncertainties. Error bars (SE) are at the 2σ level of uncertainty.

composition. Although $^{143}Nd/^{144}Nd$ ratios range from 0.512291 ± 25 (2SD, n = 10) to 0.512314 ± 66 (2SD, n = 21) there is larger scatter in the corresponding $^{147}Sm/^{144}Nd$ ratios which range from 0.1168 ± 33 (2SD, n = 18) to 0.1211 ± 30 (2SD, n = 21). The mean $^{145}Nd/^{144}Nd$ ratio of 0.348412 ± 37 (2SD, n = 73) is consistent with the recommended value of 0.348415 (Table 3). Additionally, Nd separated from the seven fragments of UWA-1 mentioned above yielded a mean $^{143}Nd/^{144}Nd$ ratio of 0.512286 ± 09 (2SD, n = 7) (Table 4, Fig. 4d) and a $^{147}Sm/^{144}Nd$ ratio of 0.1187 ± 14 (2SD, n = 6). The $\varepsilon_{Nd(t)}$ value for UWA-1 apatite is + 13.8 ± 0.3 (2SD, n = 6), which is within analytical uncertainty of the $\varepsilon_{Nd(t)}$ value of + 13.9 ± 1.5 (2SD, n = 73) obtained by LA-MC-ICP-MS analyses (Table 3, Fig. 4d).

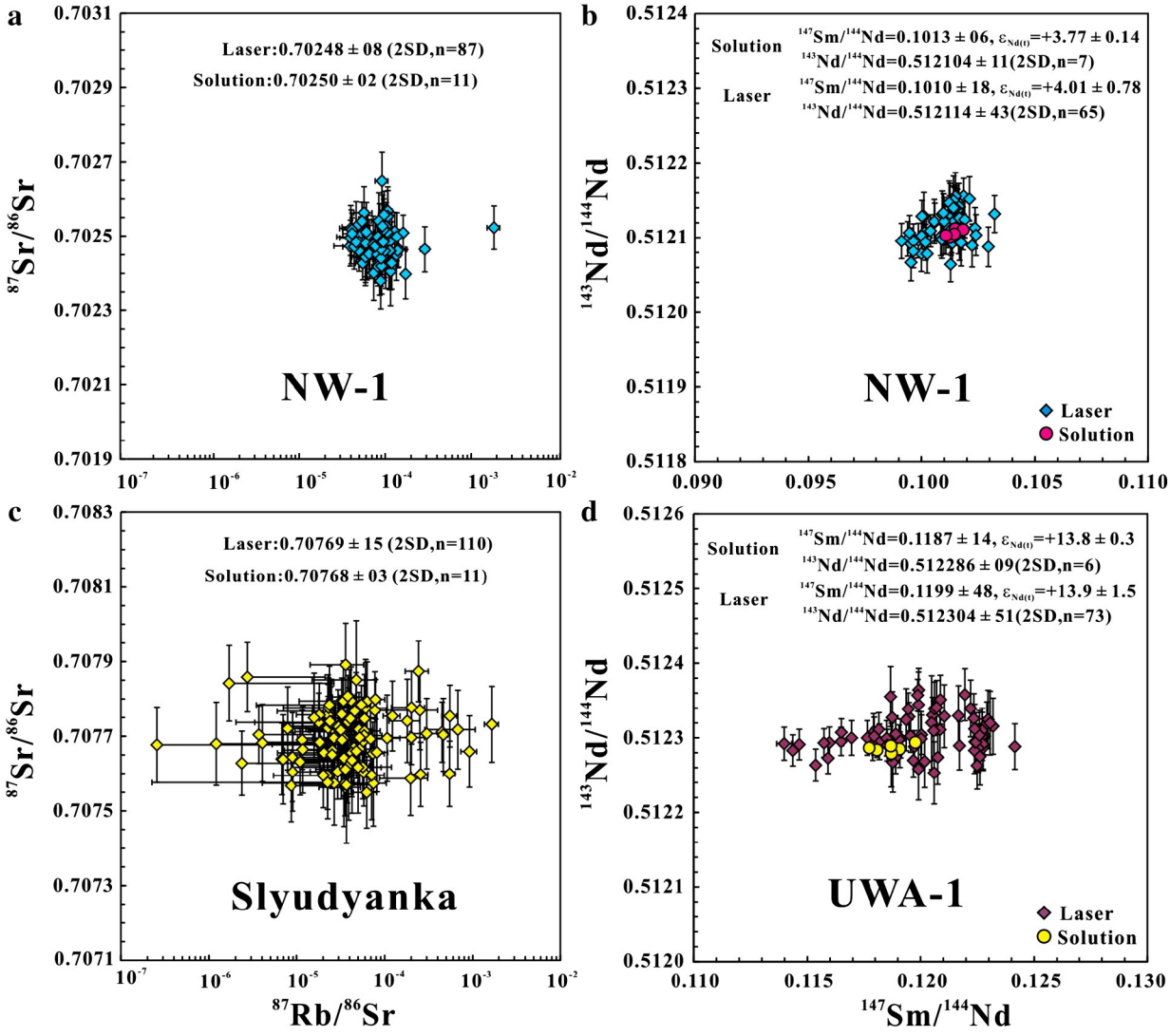

Fig. 4. Summary of measured Sr and Sm–Nd isotopic data for NW-1 (a, b), Slyudyanka (c) and UWA-1 (d) apatites analyzed using LA-MC-ICP-MS in different analytical sessions and compared to isotope-dilution MC-ICP-MS data. The laser analyses exhibit more scatter and larger uncertainties, while the solution method uncertainties are smaller than the symbols. Error bars (SE) are at the 2σ level of uncertainty.

3.8. Mud Tank apatite

Apatite megacrysts occur within the Mud Tank Carbonatite, in the Strangways Ranges of the Northern Territory NE of Alice Srings, Australia. A zircon U–Pb age of 732 ± 5 Ma and a whole-rock Rb–Sr age of 735 ± 75 Ma has been reported by Black and Gulson (1978) while younger Rb–Sr biotite ages between 319 and 349 Ma have been interpreted as representing overprinting during the Alice Springs Orogeny (Haines et al., 2001). Large centimeter to decimeter-sized Mud Tank apatite is found in the same deposit, and has been used as a calibration reference material in (U–Th)/He and fission track dating (Green et al., 2006; Spiegel et al., 2009). The Mud Tank apatite crystal investigated in this study was supplied by Barry P. Kohn. The U–Pb age of ~460 Ma for Mud Tank apatite is the reference age adopted in this study (Thomson et al., 2012). The Sr, Sm and Nd concentration estimates by LA-ICP-MS are 2681, 93 and 550 ppm respectively (Table 1). Mud Tank is LREE enriched and does not exhibit a Eu anomaly (Fig. 1a).

One LA-MC-ICP-MS session yielded an $^{87}Sr/^{86}Sr$ ratio of 0.70302 ± 8 (2SD, n = 15) (Table 2), which is consistent with the solution mean value of 0.70301 ± 3 (2SD, n = 5) of five chip aliquots selected at random (Table 4, Fig. 5a). The mean $^{84}Sr/^{86}Sr$ and $^{84}Sr/^{88}Sr$ ratios of 0.0563 ± 4 (2SD, n = 15) and 0.00673 ± 5 (2SD, n = 15), respectively, agree well with the recommended values of 0.0565 and 0.00675 (Bizzarro et al., 2003; Ramos et al., 2004; Woodhead et al., 2005; Yang et al., 2011c, 2012) (Table 2).

The average $^{143}Nd/^{144}Nd$ ratio of Mud Tank apatite was 0.512361 ± 111 (2SD, n = 15) over the course of one LA-MC-ICP-MS session, while the mean $^{147}Sm/^{144}Nd$ ratio was 0.1012 ± 4 (2SD, n = 15). The mean $^{145}Nd/^{144}Nd$ ratio of 0.348386 ± 64 (2SD, n = 15) is consistent with published values (Table 3). Additionally, the five chip aliquots yielded a mean $^{143}Nd/^{144}Nd$ ratio of 0.512385 ± 13 (2SD, n = 5) (Table 4, Fig. 5b) and a mean $^{147}Sm/^{144}Nd$ value of 0.1005 ± 16 (2SD, n = 5). The corresponding $\varepsilon_{Nd(t)}$ value for Mud Tank apatite is + 0.76 ± 0.16 (2SD, n = 5), which is within uncertainty of the LA-MC-ICP-MS value of + 0.25 ± 2.15 (2SD, n = 15) (Table 3, Fig. 5b). There is close agreement between the solution-based and LA-MC-ICP-MS analyses. Mud Tank apatite appears to exhibit a relatively large spread in $^{143}Nd/^{144}Nd$ ratios while the range in $^{87}Sr/^{86}Sr$ ratios is significantly smaller.

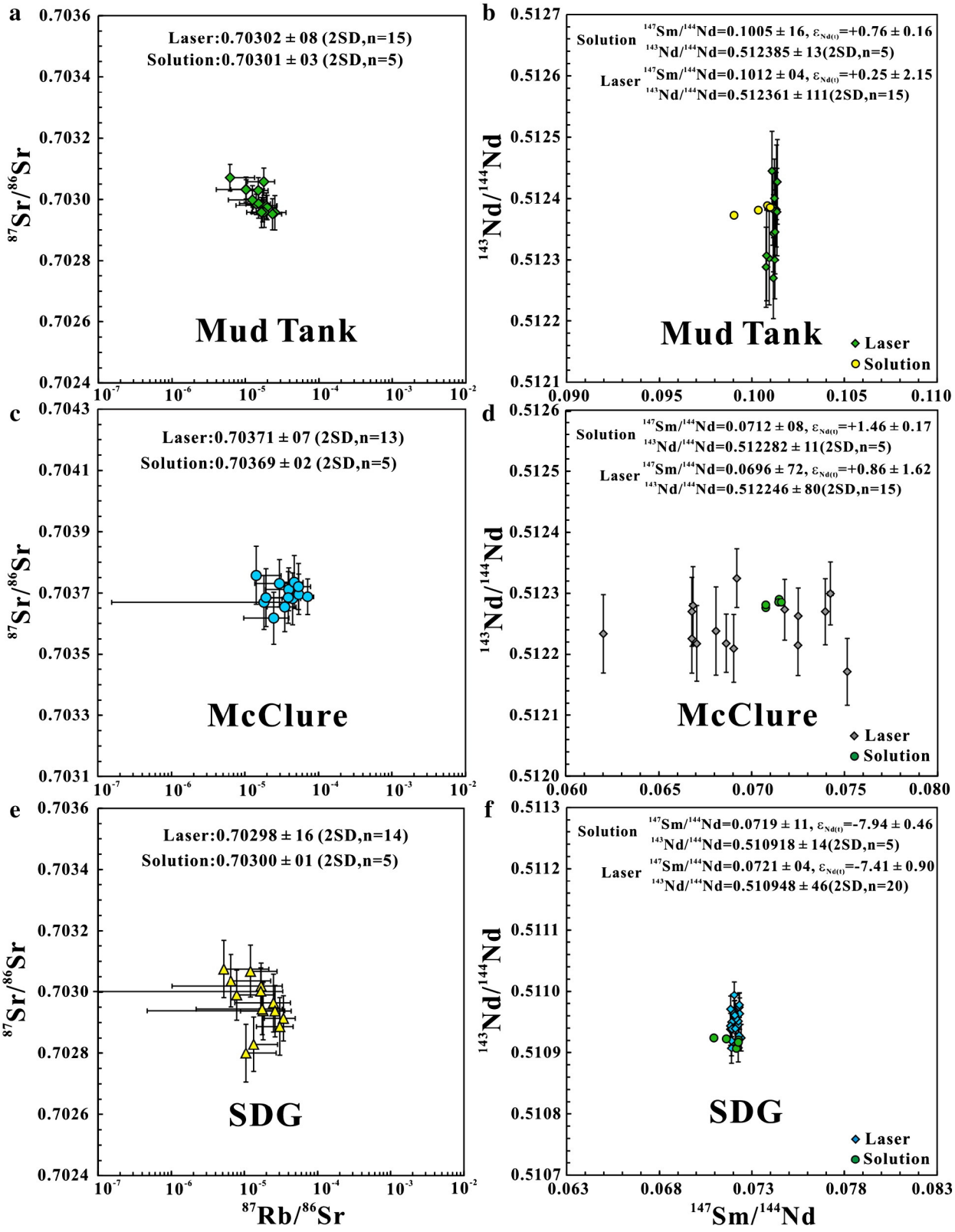

Fig. 5. Summary of measured Sr and Sm–Nd isotopic data for Mud Tank (a, b), McClure Mountain (c, d) and SDG (e, f) apatites analyzed using LA-MC-ICP-MS in different analytical sessions and compared to solution MC-ICP-MS data. The laser analyses are significantly scattered with larger uncertainties, while the solution method uncertainties are small than the symbols. Error bars (SE) are at the 2σ level of uncertainty.

3.9. McClure Mountain apatite

The Cambrian McClure Mountain syenite of Colorado is the source of the widely used $^{40}Ar/^{39}Ar$ hornblende reference material MMhb-1. Apatite from the McClure Mountain syenite occurs as small euhedral grains of apatite varying from about 500 μm to less than 50 μm in axial length. The U–Pb age of ~523.5 Ma (Schoene and Bowring, 2006) for McClure Mountain apatite is the reference age adopted in our work. The McClure Mountain apatite mineral separate investigated in this study was also supplied by D.M. Chew and was originally collected by Ray Donelick. The Sr, Sm and Nd concentration estimates by LA-ICP-MS are 3422, 102 and 843 ppm respectively (Table 1). McClure Mountain apatite is LREE enriched and exhibits a slight Eu positive anomaly (Fig. 1a).

One LA-MC-ICP-MS session yielded an $^{87}Sr/^{86}Sr$ ratio of 0.70371 ± 7 (2SD, n = 13) (Table 2), which is consistent with the solution MC-ICP-MS average value of 0.70369 ± 2 (2SD, n = 5) (Table 4, Fig. 5c). The mean $^{84}Sr/^{86}Sr$ and $^{84}Sr/^{88}Sr$ ratios of 0.0563 ± 4 (2SD, n = 13) and 0.00673 ± 5 (2SD, n = 15), respectively, agree well with the recommended values of 0.0565 and 0.00675 (Bizzarro et al., 2003; Ramos et al., 2004; Woodhead et al., 2005; Yang et al., 2011c, 2012) (Table 2).

The mean $^{143}Nd/^{144}Nd$ ratio of McClure Mountain apatite was 0.512246 ± 80 (2SD, n = 15) over the course of one LA-MC-ICP-MS session, while the mean $^{147}Sm/^{144}Nd$ ratio was 0.0696 ± 72 (2SD, n = 15). The mean $^{145}Nd/^{144}Nd$ ratio of 0.348394 ± 43 (2SD, n = 15) is consistent with published values (Table 3). Additionally, five aliquots derived from crushing grains of McClure Mountain apatite were selected at random for solution analyses, yielding a mean $^{143}Nd/^{144}Nd$ ratio of 0.512282 ± 11 (2SD, n = 5) (Table 4, Fig. 5d) and a mean $^{147}Sm/^{144}Nd$ value of 0.0712 ± 8 (2SD, n = 5). The corresponding $\varepsilon_{Nd(t)}$ value for McClure Mountain apatite is +1.46 ± 0.17 (2SD, n = 5), which is within uncertainty of the laser ablation value of +0.86 ± 1.62 (2SD, n = 15) (Table 3, Fig. 5d). McClure Mountain apatite appears to exhibit a relatively large spread in $^{143}Nd/^{144}Nd$ ratios while it has a relatively homogeneous Sr isotopic composition.

3.10. SDG apatite

The SDG apatite reference material consists of pale yellow grains that occur within an alkaline ultrabasic complex in Sandaogou in Inner Mongolia, China. It is employed as an *in-house* U–Pb dating reference material in the MC-ICP-MS laboratory of the Tianjin Institute of Geology and Mineral Resources, China Geological Survey (Zhou et al., 2012). The weighted mean $^{206}Pb/^{238}U$ age of 1602 ± 13 Ma (95% confidence, MSWD = 0.58, n = 5) obtained by ID-TIMS dating (Zhou et al., 2012) was adopted as the reference age for the initial Nd calculation in this study. The Sr, Sm and Nd concentration estimates by LA-ICP-MS are 11368, 911 and 7344 ppm respectively (Table 1). REE analysis indicates that SDG is LREE enriched and does not exhibit a Eu anomaly (Fig. 1a).

One LA-MC-ICP-MS session yielded a $^{87}Sr/^{86}Sr$ ratio of 0.70298 ± 16 (2SD, n = 14) (Table 2), which is consistent with the solution MC-ICP-MS average value of 0.70300 ± 01 (2SD, n = 5) (Table 4, Fig. 5e). The mean $^{84}Sr/^{86}Sr$ and $^{84}Sr/^{88}Sr$ ratios of 0.0564 ± 7 (2SD, n = 14) and 0.00673 ± 8 (2SD, n = 14), respectively, agree well with the recommended values of 0.0565 and 0.00675 (Bizzarro et al., 2003; Ramos et al., 2004; Woodhead et al., 2005; Yang et al., 2011c, 2012) (Table 2).

The mean $^{143}Nd/^{144}Nd$ ratio of SDG apatite was 0.510948 ± 46 (2SD, n = 20) over the course of one LA-MC-ICP-MS session, while the average $^{147}Sm/^{144}Nd$ ratio was 0.0721 ± 4 (2SD, n = 20). The mean $^{145}Nd/^{144}Nd$ ratio of 0.348405 ± 22 (2SD, n = 20) is consistent with published values (Table 3). Additionally, five aliquots derived from crushing chips of SDG apatite were selected at random for solution analyses, yielding a mean $^{143}Nd/^{144}Nd$ ratio of 0.510918 ± 14 (2SD, n = 5) (Table 4, Fig. 5f) and a mean $^{147}Sm/^{144}Nd$ value of 0.0719 ± 11 (2SD, n = 5). The corresponding $\varepsilon_{Nd(t)}$ value for SDG apatite is −7.94 ± 0.46 (2SD, n = 5), which is within uncertainty of the laser ablation value of −7.41 ± 0.90 (2SD, n = 20) (Table 3, Fig. 5f). There is close agreement between the solution-based and LA-MC-ICP-MS analyses, while SDG apatite appears relatively homogenous in terms of its Sr and Sm–Nd isotopic compositions and hence could make a promising reference material for *in situ* Sr or Nd analyses.

4. Discussions

4.1. Potential criteria of in situ Sr or Nd isotopic analysis of apatite

Low element concentrations and isobaric interferences precluded LA-MC-ICP-MS Sr or Nd isotopic analyses on some apatite samples. For *in situ* Sr measurements, our previous work demonstrated that ~500 ppm Sr is sufficient to yield an absolute precision of ±0.0001 on the $^{87}Sr/^{86}Sr$ ratio when using a large (100–160 μm) laser spot size (Yang et al., 2009b). The extremely low Rb contents (and hence very low Rb/Sr ratios) of apatite mean that isobaric interference of ^{87}Rb on ^{87}Sr is usually insignificant and can be easily accounted for (Yang et al., 2011c). As most apatite yields moderate Sr concentrations, there is usually sufficient Sr for high-precision Sr isotopic analysis. However, apatite typically exhibits high REE concentrations. A low HREE/Sr ratio (*e.g.* Er/Sr or Yb/Sr) is required for *in situ* Sr analyses due to double-charged ion interference on ^{84}Sr and ^{86}Sr. As shown in Fig. 6, Er double-charged ions dominate over Yb double-charged ions as isobaric interferences on Sr isotope data because Er is more susceptible to double-charged ion formation (Yang et al., 2012, 2014b). Our experience indicates that Er/Sr or Yb/Sr ratios should be lower than ~0.1 to obtain reliable *in situ* Sr isotopic analyses of apatite (Wu et al., 2010a,b,c). Therefore using these criteria, UWA-1 apatite with its elevated HREE contents and HREE/Sr ratios (Er/Sr = 0.35 or Yb/Sr = 0.26) is not suitable for *in situ* Sr analysis.

With regard to *in situ* Nd isotopic analyses, only Slyudyanka apatite (~53 ppm Nd) was not suitable for Nd isotopic analysis in this study (Table 1). As shown in Fig. 7, SRM NIST 610 was ablated using a 160 μm spot size with an 8 Hz repetition rate yielding a mean $^{143}Nd/^{144}Nd$ ratio of 0.511931 ± 67 (2SD, n = 40), which is comparable with the reported valued of 0.511927 ± 4 (2SE) by ID-TIMS (Woodhead and Hergt, 2001), and also agrees well with a recently reported value of 0.511921 ± 13 (2SE, n = 70) determined by LA-MC-ICP-MS (Kimura et al., 2013a). A sufficiently high Nd concentration in the target material and a Sm/Nd ratio of less than *ca.* 1 ($^{147}Sm/^{144}Nd < 0.63$) are the two prerequisites for accurate and precise *in situ* Nd LA-MC-ICP-MS analyses

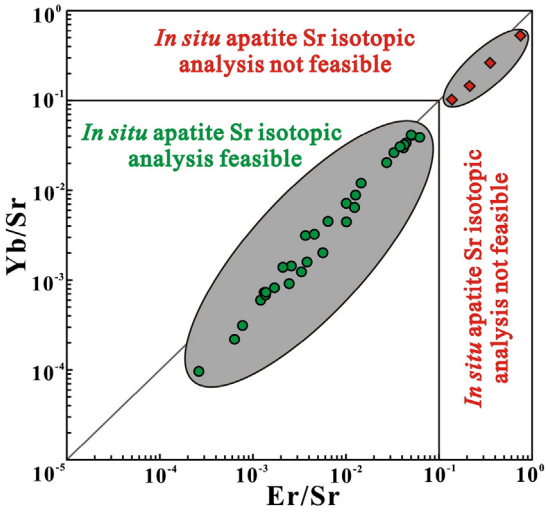

Fig. 6. Er/Sr and Yb/Sr variation diagram showing the compositional range for obtaining accurate Sr isotopic compositions for apatite using the LA-MC-ICP-MS method. The error bars are significantly smaller than the symbols and are not shown.

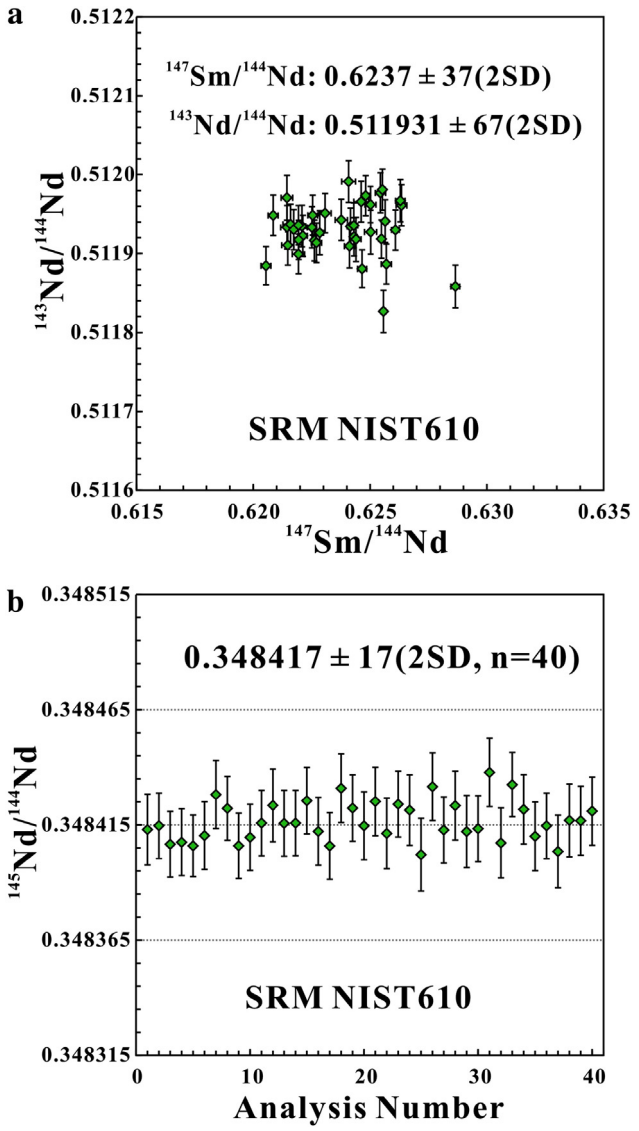

Fig. 7. Nd isotope composition of SRM NIST 610 standard glass by laser ablation analysis (160 μm spot size with an 8 Hz repetition rate). All error bars are at the 2σ level of uncertainty.

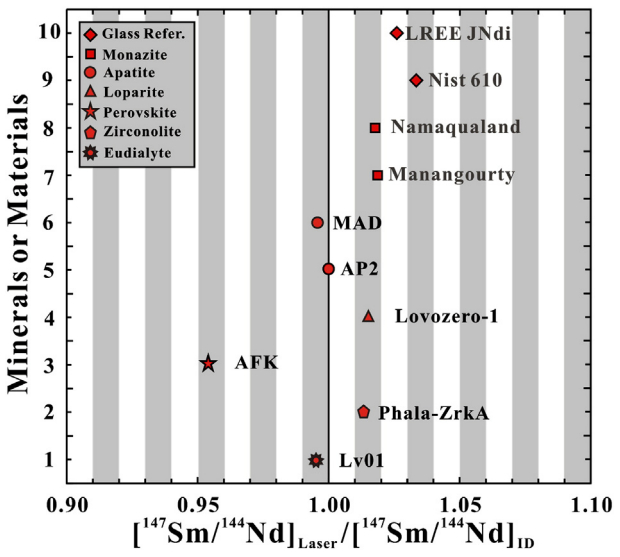

Fig. 8. Laser-ablation $^{147}Sm/^{144}Nd$ ratios for different minerals or standard glass reference materials obtained by external calibration with $^{147}Sm/^{144}Nd$ (ID method) value of AP2 apatite reference material (measured during the same analytical session), compared with the isotope-dilution $^{147}Sm/^{144}Nd$ ratios of these materials. A matrix-matched reference material method is clearly required to calculate absolute $^{147}Sm/^{144}Nd$ ratios. Gray rectangles denote a ~1% range in the horizontal axis, indicating that there are insignificant $^{147}Sm/^{144}Nd$ (~1%) variations between the LA-MC-ICP-MS and ID methods for the same minerals or materials used in the external calibration, while the discrepancy on the $^{147}Sm/^{144}Nd$ ratio between the LA-MC-ICP-MS and ID methods is significantly larger (between 2% to 5%) when AP2 was used to externally calibrate other minerals or materials.

(Foster and Vance, 2006; Yang et al., 2008). Additionally, our calculated corresponding $\varepsilon_{Nd(t)}$ values from the LA-MC-ICP-MS data closely match those obtained by solution analyses (Tables 3, 4 and 6). The data presented in this study demonstrate that reliable Sr and Nd isotopic compositions can be obtained for the majority of natural apatite samples by LA-MC-ICP-MS.

4.2. A matrix-matched calibration for in situ Sr or Nd analysis of apatite

Interference-corrected LA-MC-ICP-MS $^{87}Sr/^{86}Sr$ data of apatite are generally considered to represent the apatite initial Sr isotopic composition because of its inherently low Rb/Sr ratio (Figs. 2, 3, 4, 5 and Table 2). However, unlike for *in situ* Sr analysis, $^{143}Nd/^{144}Nd$ isotopic analyses require precise and accurate determination of the parent to daughter elemental ratio (*e.g.*, $^{147}Sm/^{144}Nd$) in order to obtain the initial $^{143}Nd/^{144}Nd$ ratio (and also initial ε_{Nd} values) (Liu et al., 2012; Fisher et al., 2011b; Iizuka et al., 2011; Yang et al., 2013; Kimura et al., 2013a,b). In order to reduce the matrix effect between different mineral samples during laser ablation analyses, we typically employed two in-house apatite reference materials during analytical sessions. As demonstrated in Fig. 8, there are insignificant $^{147}Sm/^{144}Nd$ (~1%) variations between the LA-MC-ICP-MS and ID methods for the same minerals or materials used in the external calibration, while the discrepancy on the $^{147}Sm/^{144}Nd$ ratio between the LA-MC-ICP-MS and ID methods is significantly larger (between 2% to 5%) when AP2 was used to externally calibrate other minerals or materials (*e.g.* perovskite). Therefore, an external apatite reference material is necessary for simultaneous $^{147}Sm/^{144}Nd$ and $^{143}Nd/^{144}Nd$ measurements by laser ablation MC-ICP-MS (Foster and Vance, 2006; Fisher et al., 2011b; Iizuka et al., 2011; Kimura et al., 2013a; Yang et al., 2009a, 2013; Sarkar et al., 2014). In this study, we used an apatite reference material rather than a synthetic reference material (such as standard glass) for external calibration. As shown in Table 3 and Figs. 2, 3, 4 and 5, the obtained $^{147}Sm/^{144}Nd$ and $^{143}Nd/^{144}Nd$ ratios of the apatite samples agree well with the values obtained by solution-based methods, which confirms the reliability of our *in situ* protocol for simultaneous determinations of $^{147}Sm/^{144}Nd$ and $^{143}Nd/^{144}Nd$ ratios.

4.3. Candidate reference materials for in situ Sr and Nd isotopic analyses of apatite

Generally speaking, candidate apatite reference materials for *in situ* Sr or Nd isotopic analyses by LA-MC-ICP-MS should have the following requirements: (1) the Sr or Nd isotopic composition should be homogenous both within and between individual grains; (2) they should contain moderate (and preferably homogenous) Sr or Nd concentrations; (3) they should exhibit low Er/Sr and Yb/Sr (HREEs) values for Sr isotopic analyses to minimize double-charged ion isobaric interference; (4) a knowledge of the crystallization age (*e.g.* U–Th–Pb dates) is required for Nd isotopic analyses so the initial Nd isotopic composition (and ε_{Nd} values) can be calculated; (5) they should be readily available, ideally as large crystals in sufficient quantity to supply the scientific community. Based on the *in situ* measurements of Sr and Nd isotopic compositions of eleven apatite reference materials commonly used in U–Th–Pb geochronology we suggest that AP1, MAD, Otter Lake, NW-1, Slyudyanka, Mud Tank, McClure Mountain and SDG apatite make good potential candidates for *in situ* Sr

isotopic analyses, while AP1, AP2, MAD, Otter Lake, NW-1 and SDG are potential candidates for *in situ* Nd isotopic analyses.

Additionally, as shown in Fig. 9, the four Durango apatites analyzed are inhomogeneous in terms of their $^{147}Sm/^{144}Nd$ ratios despite exhibiting uniform $^{143}Nd/^{144}Nd$ ratios during the same analytical sessions. Similarly, Table 2 demonstrates that the Durango_Fisher crystal is clearly different in its trace element composition compared to the other three Durango (Chew, Griffin and Hou) apatite crystals. This demonstrates that Durango apatite is inhomogeneous in terms of its Sm/Nd ratio, a conclusion that was also reached by Foster and Vance (2006) and Fisher et al. (2011b) (Table 6). Therefore, Durango apatite is not a promising candidate for an apatite reference material for Sm/Nd ratio determinations by LA-MC-ICP-MS despite yielding homogeneous $^{143}Nd/^{144}Nd$ data (Fig. 9).

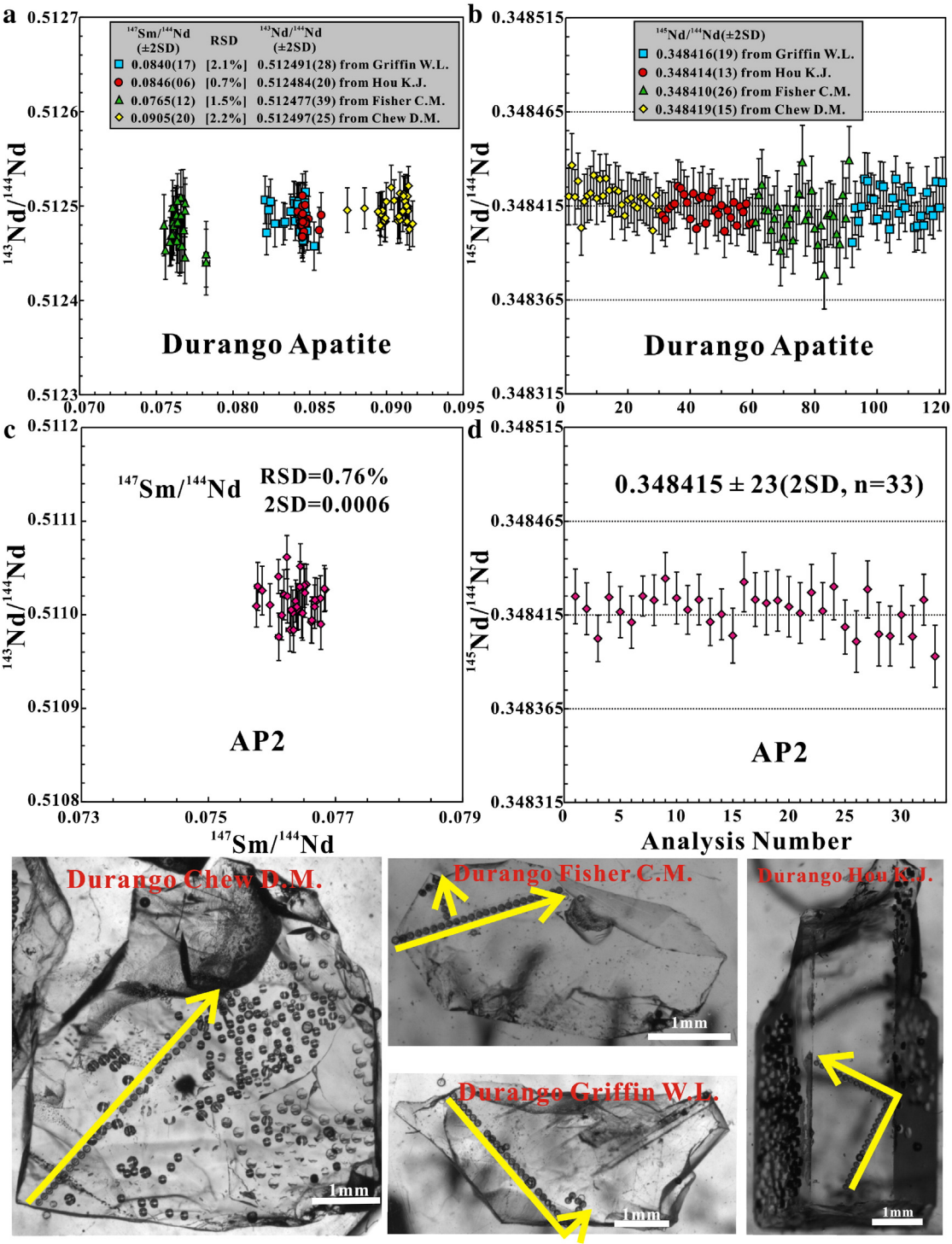

Fig. 9. Sm–Nd isotope laser ablation analyses of Durango apatite (90 μm spot size with an 8 Hz repetition rate) during one analytical session, indicating the significant variation in $^{147}Sm/^{144}Nd$ ratio in different Durango apatite crystals, while our in-house AP2 apatite reference material yields homogenous $^{147}Sm/^{144}Nd$ data during the same analytical session. All error bars are at the 2σ level of uncertainty.

5. Conclusions

Considering the need for apatite reference materials for *in situ* Sr or Nd isotopic analyses, we undertook both laser ablation and solution-based measurements of the Sr and Nd isotopic compositions of eleven potential apatite reference materials (AP1, AP2, Durango, MAD, Otter Lake, NW-1, Slyudyanka, UWA-1, Mud Tank, McClure Mountain and SDG) that have been extensively used and distributed in U–Th–Pb geochronology studies. Our obtained Sr and Nd isotopic compositions for natural apatite samples are all consistent with those values obtained by solution-based methods (both ID-MC-ICP-MS and ID-TIMS).

During *in situ* Sr analyses of apatite, isobaric interference from HREE on ^{84}Sr and ^{86}Sr can be significant. Importantly, Er double-charged ions dominate over Yb double-charged ions as isobaric interferences on Sr isotopes because Er is more prone to double-charged ion formation. Our work indicates that Er/Sr or Yb/Sr ratios greater than 0.1 combined with low Sr contents, make it impossible to obtain reliable $^{87}Sr/^{86}Sr$ data by LA-MC-ICP-MS. Interferences from Kr (in the carrier gas) and Rb (present in very small quantities in most apatite crystals) are usually insignificant and can be easily corrected by using our analytical protocol. A matrix-matched apatite reference material is recommended for external calibration of $^{87}Sr/^{86}Sr$ ratios.

AP1, MAD, Otter Lake, NW-1, Slyudyanka, Mud Tank, McClure Mountain and SDG apatites are relatively homogeneous in terms of their Sr isotopic compositions, while AP1, AP2, MAD, Otter Lake, NW-1 and SDG apatites are relatively uniform in terms of their Sm–Nd isotopic compositions. However, UWA-1 apatite is not promising reference material for either *in situ* Sr or Nd isotopic analyses, while Durango apatite is not a promising candidate apatite reference material for Sm/Nd ratio determinations by LA-MC-ICP-MS despite yielding homogeneous $^{143}Nd/^{144}Nd$ data.

Acknowledgments

This work was financially supported by the Natural Science Foundation of China (Grants 41221002, 41273021 and 41130313) and the State Key Laboratory of Lithospheric Evolution (Grant 0806). Wei-Qiang Ji, Zhi-Chao Liu, Qin Zhou, Jin-Feng Sun, Yu-Sheng, Zhu, Jing Sun, Jing-Yuan Chen, Lin-Min Zhang, Chang Zhang and Yang Li are thanked for their assistance during sample preparation and analytical sessions. Drs Zhi-Li Qiu, Roger Mitchell, Stuart N. Thomson, John W. Valley, Barry P. Kohn and Ke-Qing Zong kindly provided the AP1 & AP2, NW-1, MAD, UWA-1, Mud Tank and SDG apatite reference materials respectively which was most appreciated. Detailed comments from Editor Laurie Reisberg and the constructive suggestions of Chris Fisher and an anonymous referee are gratefully acknowledged and significantly improved the manuscript. We are willing to distribute these apatite reference materials to other laboratories upon request.

References

Adams, C.J., Campbell, H.J., Griffin, W.L., 2005. Isotopic microanalysis of seawater strontium in biogenic calcite to assess subsequent rehomogenisation during metamorphism. Chem. Geol. 220, 67–82.

Amelin, Y., 2005. Meteorite phosphates show constant ^{176}Lu decay rate since 4557 million years ago. Science 310, 839–841.

Balcaen, L., De Schrijver, I., Moens, L., Vanhaecke, F., 2005. Determination of the $^{87}Sr/^{86}Sr$ isotope ratio in USGS silicate reference materials by multi-collector ICP–mass spectrometry. Int. J. Mass Spectrom. 242, 251–255.

Balter, V., Telouk, P., Reynard, B., Braga, J., Thackeray, F., Albarede, F., 2008. Analysis of coupled Sr/Ca and $^{87}Sr/^{86}Sr$ variations in enamel using laser-ablation tandem quadrupole-multicollector ICPMS. Geochim. Cosmochim. Acta 2008 (72), 3980–3990.

Barfod, G.H., Albarede, F., Knoll, A.H., Xiao, S., Telouk, P., Frei, R., Baker, J.A., 2002. New Lu–Hf and Pb–Pb age constraints of the earliest animal fossils. Earth Planet. Sci. Lett. 201, 203–212.

Barfod, G.H., Otero, O., Albarede, F., 2003. Phosphate Lu–Hf geochronology. Chem. Geol. 200, 241–253.

Barfod, G.H., Krogstad, E.J., Frei, R., Albarede, F., 2005. Lu–Hf and PbSL geochronology of apatites from Proterozoic terranes: a first look at Lu–Hf isotopic closure in metamorphic apatite. Geochim. Cosmochim. Acta 69, 1847–1859.

Belousova, E.A., Walters, S., Griffin, W.L., O'Reilly, S.Y., 2001. Trace-element signatures of apatites in granitoids from the Mt Isa Inlier, northwestern Queensland. Aust. J. Earth Sci. 48, 603–619.

Belousova, E.A., Griffin, W.L., O'Reilly, S., Fisher, N.I., 2002. Apatite as an indicator mineral for mineral exploration: trace-element compositions and their relationship to host rock type. J. Geochem. Explor. 76, 45–69.

Bizzarro, M., Simonetti, A., Stevenson, R.K., Kurszlaukis, S., 2003. In situ $^{87}Sr/^{86}Sr$ investigation of igneous apatites and carbonates using laser-ablation MC-ICP-MS. Geochim. Cosmochim. Acta 67, 289–302.

Black, L.P., Gulson, B.L., 1978. The age of the Mud Tank carbonatite, Strangways Range, Northern Territory. Bureau of Mineral Resources. J. Aust. Geol. Geophys. 3, 227–232.

Blichert-Toft, J., 2008. The Hf isotopic composition of zircon reference material 91500. Chem. Geol. 253, 252–257.

Carter, A., Foster, G.L., 2009. Improving constraints on apatite provenance: Nd measurement on fission-track-dated grains. Geol. Soc. Lond. Spec. Publ. 324, 57–72.

Chartier, F., Aubert, M., Salmon, M., Tabarant, M., Tran, B.H., 1999. Determination of erbium in nuclear fuels by isotope dilution thermal ionization mass spectrometry and glow discharge mass spectrometry. J. Anal. At. Spectrom. 14, 1461–1465.

Chew, D.M., Sylvester, P.J., Tubrett, M.N., 2011. U–Pb and Th–Pb dating of apatite by LA–ICPMS. Chem. Geol. 280, 200–216.

Chew, D.M., Petrus, J.A., Kamber, B.S., 2014. U–Pb LA-MC-ICP-MS dating using accessory mineral standards with variable common Pb. Chem. Geol. 363, 185–199.

Christensen, J.N., Halliday, A.N., Lee, D.C., Hall, C.M., 1995. *In situ* Sr isotopic analysis by laser ablation. Earth Planet. Sci. Lett. 136, 79–85.

Chu, M.F., Wang, K.L., Griffin, W.L., Chung, S.L., O'Reilly, S.Y., Pearson, N.J., Lizuka, Y., 2009a. Apatite composition: tracing petrogenetic processes in Transhimalayan granitoids. J. Petrol. 50, 1829–1855.

Chu, Z.Y., Chen, F.K., Yang, Y.H., Guo, J.H., 2009b. Precise determination of Sm, Nd concentrations and Nd isotopic compositions at the nanogram level in geological samples by thermal ionization mass spectrometry. J. Anal. At. Spectrom. 24, 1534–1544.

Copeland, S.R., Sponheimer, M., le Roux, P.J., Grimes, V., Lee-Thorp, J.A., de Ruiter, D.J., Richards, M.P., 2008. Strontium isotope ratios ($^{87}Sr/^{86}Sr$) of tooth enamel: a comparison of solution and laser ablation multicollector inductively coupled plasma mass spectrometry methods. Rapid Commun. Mass Spectrom. 22, 3187–3194.

Copeland, S.R., Sponheimer, M., Lee-Thorp, J.A., le Roux, P.J., de Ruiter, D.J., Richards, M.P., 2010. Strontium isotope ratios in fossil teeth from South Africa: assessing laser ablation MC-ICP-MS analysis and the extent of diagenesis. J. Archaeol. Sci. 37, 1437–1446.

Dempster, T.J., Jolivet, M., Tubrett, M.N., Braithwaite, C.J.R., 2003. Magmatic zoning in apatite: a monitor of porosity and permeability change in granites. Contrib. Mineral. Petrol. 145 (5), 568–577.

Dubois, J.C., Retali, G., Cesario, J., 1992. Isotopic analysis of rare earth elements by total vaporization of samples in thermal ionization mass spectrometry. Int. J. Mass Spectrom. 120, 163–177.

Ehrlich, S., Gavrieli, I., Dor, L.B., Halicz, L., 2001. Direct high-precision measurements of the $^{87}Sr/^{86}Sr$ isotope ratio in natural water, carbonates and related materials by multiple collector inductively coupled plasma mass spectrometry (MC-ICP-MS). J. Anal. At. Spectrom. 16, 1389–1392.

Fietzke, J., Liebertrau, V., Gunther, D., Gurs, K., Hametner, K., Zumholz, K., Hansteen, T.H., Eisenhauer, A., 2008. An alternative data acquisition and evaluation strategy for improved isotope ratio precision using LA-MC-ICP-MS applied to stable and radiogenic strontium isotopes in carbonates. J. Anal. At. Spectrom. 23, 955–961.

Fisher, Christopher M., Hanchar, John M., Samson, Scott D., Dhuime, Bruno, Blichert-Toft, Janne, Vervoort, Jeffery D., Lam, Rebecca, 2011a. Synthetic zircon doped with hafnium and rare earth elements: a reference material for in situ hafnium isotope analysis. Chem. Geol. 286, 32–47.

Fisher, Christopher M., McFarlane, Christopher R.M., Hanchar, John M., Schmitz, Mark D., Sylvester, Paul J., Lam, Rebecca, Longerich, Henry P., 2011b. Sm–Nd isotope systematics by laser ablation-multicollector-inductively coupled plasma mass spectrometry: methods and potential natural and synthetic reference materials. Chem. Geol. 284, 1–20.

Fortunato, G., Mumic, K., Wunderli, S., Pillonel, L., Bosset, J.O., Gremand, G., 2004. Application of strontium isotope abundance ratios measured by MC-ICP-MS for food authentication. J. Anal. At. Spectrom. 19, 227–234.

Foster, G.L., Carter, A., 2007. Insights into the patterns and locations of erosion in the Himalaya—a combined fission-track and *in situ* Sm–Nd isotopic study of detrital apatite. Earth Planet. Sci. Lett. 257, 407–418.

Foster, G.L., Vance, D., 2006. *In situ* Nd&& isotopic analysis of geological materials by laser ablation MC-ICP-MS. J. Anal. At. Spectrom. 21, 288–296.

Frei, D., Harlov, D., Dulski, P., Ronsbo, J., 2005. Apatite from Durango (Mexico) — a potential standard for *in situ* trace element analysis of phosphates. Geochim. Cosmochim. Acta 69, A794.

Goldstein, S.L., Onions, R.K., Hamilton, P.J., 1984. A Sm–Nd isotopic study of atmospheric dusts and particulates from major river systems. Earth Planet. Sci. Lett. 70, 221–236.

Green, P.F., Crowhurst, P.V., Duddy, I.R., Japsen, T., Holford, S.P., 2006. Conflicting (U–Th)/He and fission track ages in apatite: enhanced He retention, not anomalous annealing behaviour. Earth Planet. Sci. Lett. 250 (3–4), 407–427.

Gregory, C.J., McFarlane, C.R.M., Hermann, J., Rubatto, D., 2009. Tracing the evolution of calc-alkaline magmas: in-situ Sm–Nd isotope studies of accessory minerals in the Bergell igneous complex, Italy. Chem. Geol. 260, 73–86.

Griffin, W.L., Powell, W.J., Pearson, N.J., O'Reilly,, S.Y., 2008. GLITTER: data reduction software for laser ablation ICP-MS. In: Sylvester, P. (Ed.), Laser ablation-ICP-MS in the Earth Sciences: current practices and outstanding issues. Mineralogical Association Canada Short Course, 40, pp. 308–311.

Guo, S., Ye, K., Yang, Y.H., Chen, Y., Zhang, L.M., Liu, J.B., Mao, Q., Ma, Y.G., 2014. In situ Sr isotopic analyses of epidote: tracing the sources of multi-stage fluids in ultrahigh-pressure eclogite (Ganghe, Dabie terrane). Contrib. Mineral. Petrol. 16, 975.
Haines, P.W., Hand, M., Sandiford, M., 2001. Palaeozoic synorogenic sedimentation in central and northern Australia: a review of distribution and timing with implications for the evolution of intracontinental orogens. Aust. J. Earth Sci. 48 (6), 911–928.
Hart, S.R., Ball, L., Jackson, M., 2005. Sr isotope by laser ablation PIMMS: application to CPX from Samoan Peridotite Xenoliths. WHOI Plasma Facility Open File Technical Report, 11. Woods Hole Oceanographic Institution.
Henderson, A.L., Foster, G.L., Najman, Y., 2010. Testing the application of *in situ* Sm–Nd isotopic analysis on detrital apatites: a provenance tool for constraining the timing of India–Eurasia collision. Earth Planet. Sci. Lett. 297, 42–49.
Horstwood, M.S.A., Evans, J.A., Montgomery, J., 2008. Determination of Sr isotopes in calcium phosphates using laser ablation inductively coupled plasma mass spectrometry and their application to archaeological tooth enamel. Geochim. Cosmochim. Acta 72, 5659–5674.
Hou, K.J., Qin, Y., Li, Y.H., Fan, C.F., 2013. *In situ* Sr, Nd isotopic measurement of apatite using laser ablation multi-collector inductively coupled plasma mass spectrometry (in Chinese with English abstract). Rock Miner. Anal. 32 (8), 547–554.
Iizuka, T., Eggins, S.M., McCulloch, M.T., Kinsley, L.P.J., Mortimer, G.E., 2011. Precise and accurate determination of $^{147}Sm/^{144}Nd$ and $^{143}Nd/^{144}Nd$ in monazite using laser ablation-MC-ICPMS. Chem. Geol. 282, 45–57.
Isnard, H., Brennetot, R., Caussignac, C., Caussignac, N., Chartier, F., 2005. Investigations for determination of Gd and Sm isotopic compositions in spent nuclear fuels samples by MC ICPMS. Int. J. Mass Spectrom. 246, 66–73.
Jackson, M.G., Hart, S.R., 2006. Strontium isotopes in melt inclusions from Samoan basalts: implications for heterogeneity in the Samoan plume. Earth Planet. Sci. Lett. 245, 260–277.
Jackson, S.E., Pearson, N.J., Griffin, W.L., 2001. *In situ* isotope ratio determination using laser ablation (LA)-magnetic sector-ICP-MS. In: Sylvester, P. (Ed.), Laser Ablation-ICP-MS in the Earth Sciences: Principles and Applications. Mineral. Assoc. Can. Short Course Series, 29, pp. 105–120.
Jacobsen, S.B., Wasserburg, G.J., 1980. Sm–Nd isotopic evolution of chondrites. Earth Planet. Sci. Lett. 50, 139–155.
Kimura, J.I., Chang, Q., Kawabata, H., 2013a. Standardless determination of Nd isotope ratios in glasses and minerals using laser-ablation multiple-collector inductively coupled plasma mass spectrometry with a low-oxide molecular yield interface setup. J. Anal. At. Spectrom. 28, 1522–1529.
Kimura, J.I., Takahashi, T., Chang, Q., 2013b. A new analytical bias correction for *in situ* Sr isotope analysis of plagioclase crystals using laser-ablation multiple-collector inductively coupled plasma mass spectrometry. J. Anal. At. Spectrom. 28, 945–957.
Kretz, R., Campbell, J.L., Hoffman, E.L., Hartree, R., Teesdale, W.J., 1999. Approaches to equilibrium in the distribution of trace elements among the principal minerals in a high-grade metamorphic terrane. J. Metamorph. Geol. 17, 41–59.
Li, C.F., Chen, F.K., Li, X.H., 2007. Precise isotopic measurements of sub-nanogram Nd of standard reference material by thermal ionization mass spectrometry using the NdO^+ technique. Int. J. Mass Spectrom. 266, 34–41.
Li, Q.L., Li, X.H., Wu, F.Y., Yin, Q.Z., Ye, H.M., Liu, Y., Tang, G.Q., Zhang, C.L., 2012. In-situ SIMS U–Pb dating of Phanerozoic apatite with low U and high common Pb. Gondwana Res. 21, 745–756.
Liu, Z.C., Wu, F.Y., Yang, Y.H., Yang, J.H., Wilde, S.A., 2012. Neodymium isotopic compositions of the standard monazites used in U–Th–Pb geochronology. Chem. Geol. 334, 221–239.
Lugmair, G.W., Marti, K., 1978. Lunar initial $^{143}Nd/^{144}Nd$: differential evolution of the lunar crust and mantle. Earth Planet. Sci. Lett. 39, 349–357.
McDonough, W.F., Sun, S.S., 1995. The composition of the Earth. Chem. Geol. 120, 223–253.
McDowell, F.W., McIntosh, W.C., Farley, K.A., 2005. A precise $^{40}Ar–^{39}Ar$ reference age for the Durango apatite (U–Th)/He and fission-track dating standard. Chem. Geol. 214, 249–263.
McFarlane, C.R.M., McCulloch, M.T., 2007. Coupling of in-situ Sm–Nd systematics and U–Pb dating of monazite and allanite with applications to crustal evolution studies. Chem. Geol. 245, 45–60.
McFarlane, C.R.M., McCulloch, M.T., 2008. Sm–Nd and Sr isotope systematics in LREE-rich accessory minerals using LA-MC-ICP-MS. In: Sylvester, P. (Ed.), Laser-Ablation ICPMS in the Earth Sciences: Current Practices and Outstanding Issues. Mineralogical Association of Canada Short Course, 40, pp. 117–133 (Vancouver, B.C.).
Mitchell, R.H., Wu, F.Y., Yang, Y.H., 2011. In situ U–Pb, Sr and Nd isotopic analysis of loparite by LA-(MC)-ICP-MS. Chem. Geol. 280, 191–199.
Morishita, T., Hattori, K.H., Terada, K., Matsumoto, T., Yamamoto, K., Takebe, M., Ishida, Y., Tamura, A., Arai, S., 2008. Geochemistry of apatite-rich layers in the Finero phlogopite–peridotite massif (Italian Western Alps) and ion microprobe dating of apatite. Chem. Geol. 251, 99–111.
Nishizawa, M., Terada, K., Sano, Y., Ueno, Y., 2004. Ion microprobe U–Pb dating and REE analysis of apatite from kerogen-rich silica dike from North Pole area, Pilbara Craton, Western Australia. Geochem. J. 38, 243–254.
Nowell, G.M., Horstwood, M.S.A., 2009. Comments on Richards et al., Journal of Archaeological Science 35, 2008 "Strontium isotope evidence of Neanderthal mobility at the site of Lakonis, Greece using laser-ablation PIMMS". J. Archaeol. Sci. 36, 1334–1341.
Pan, Y.M., Fleet, M.E., 2002. Compositions of the apatite-group minerals: substitution mechanisms and controlling factors. In: Kohn, M.J., Rakovan, J., Hughes, L.M. (Eds.), Phosphates: Geochemical, geobiological, and materials importance. Reviews in Mineralogy & Geochemistry, 48, pp. 13–49.
Pin, C., Zalduegui, J.F.S., 1997. Sequential separation of light rare-earth elements, thorium and uranium by miniaturized extraction chromatography: application to isotopic analyses of silicate rocks. Anal. Chim. Acta. 339, 79–89.
Poitrasson, F., Hanchar, J.M., Schaltegger, U., 2002. The current state and future of accessory mineral research. Chem. Geol. 191, 3–24.
Rakovan, J., McDaniel, D.K., Reeder, R., 1997. Use of surface-controlled REE sectoral zoning in apatite from Llallagua, Bolivia, to determine a single-crystal Sm–Nd age. Earth Planet. Sci. Lett. 146, 329–336.
Ramos, F.C., Wolff, J.A., Tollstrup, D.L., 2004. Measuring $^{87}Sr/^{86}Sr$ variation in minerals and groundmass from basalts using LA-MC-ICPMS. Chem. Geol. 211, 135–158.
Ramos, F.C., Wolff, J.A., Tollstrup, D.L., 2005. Sr isotope disequilibrium in Columbia River flood basalts: evidence for rapid shallow-level open system processes. Geology 33, 457–460.
Reznitskii, L.Z., Fefelov, N.N., Vasil'ev, E.P., Zarudneva, N.V., Nekrasova, E.A., 1998. Isotopic composition of lead from metaphosphorites and problem of the Slyudyanka Group age, the southern Baikal, Western Khamar Daban region. Lithol. Miner. Resour. 33, 432–441.
Reznitskii, L.Z., Sandimirova, G.P., Pakhol'chenko, Y.A., Kuznetsova, S.V., 1999. The Rb–Sr age of the phlogopite deposits in Slyudyanka, southern Baikal region. Dokl. Earth Sci. 367, 711–713.
Reznitskii, L.Z., et al., 2000. The age and time span of the origin of phlogopite and lazurite deposits in the southwestern Baikal area: U–Pb geochronology. Petrology 8, 66–76.
Richards, M., Harvati, K., Grimes, V., Smith, C., Smith, T., Hublin, J.J., Karkanas, P., Panagopoulou, E., 2008. Stontium isotope evidence of Neanderthal mobility at the site of Lakonis, Greece using laser-ablation PIMMS. J. Archaeol. Sci. 35, 1251–1256.
Richards, M., Grimes, V., Smith, C., Smith, T., Harvati, K., Hublin, J.J., Karkanas, P., Panagopoulou, E., 2009. Response to Nowell and Horstwood. J. Archaeol. Sci. 36, 1657–1658.
Sano, Y., Oyama, T., Terada, K., Hidaka, H., 1999. Ion microprobe U–Pb dating of apatite. Chem. Geol. 153, 249–258.
Sano, Y., Terada, K., Ly, C.V., Park, E.J., 2006. Ion microprobe U–Pb dating of a dinosaur tooth. Geochem. J. 40, 171–179.
Sarkar, C., Hawkesworth, C., Storey, C.J., 2014. Using perovskite to determine the pre-shallow level contamination magma characteristics of kimberlite. Chem. Geol. 363, 76–90.
Scherer, E., Munker, C., Mezger, K., 2001. Calibration of the lutetium–hafnium clock. Science 293, 683–687.
Schmidberger, S.S., Simonetti, A., Francis, D., 2003. Small-scale Sr isotope investigation of clinopyroxenes from peridotite xenoliths by laser ablation MC-ICP-MS — implications for mantle metasomatism. Chem. Geol. 199, 317–329.
Schoene, B., Bowring, S.A., 2006. U–Pb systematics of the McClure Mountain syenite: thermochronological constraints on the age of the 40Ar/39Ar standard McClure. Contrib. Mineral. Petrol. 151, 615–630.
Sha, L.K., Chappell, B.W., 1999. Apatite chemical composition, determined by electron microprobe and laser-ablation inductively coupled plasma mass spectrometry, as a probe into granite petrogenesis. Geochim. Cosmochim. Acta 63, 3861–3881.
Simonetti, A., Buzon, M.R., Creaser, R.A., 2008. In-situ elemental and Sr isotope investigation of human tooth enamel by laser ablation-(MC)-ICP-MS: successes and pitfalls. Archaeometry 50, 371–385.
Soderlund, U., Patchett, P.J., Vervoort, J.D., Isachsen, C.E., 2004. The ^{176}Lu decay constant determined by Lu–Hf and U–Pb isotope systematics of Precambrian mafic intrusions. Earth Planet. Sci. Lett. 219, 311–324.
Spiegel, C., Kohn, B., Belton, D., Berner, Z., Gleadow, A., 2009. Apatite (U–Th–Sm)/He thermochronology of rapidly cooled samples: the effect of He implantation. Earth Planet. Sci. Lett. 285, 105–114.
Thirlwall, M., 1991. Long-term reproducibility of multicollector Sr and Nd isotope ratio analyses. Chem. Geol. 94, 85–104.
Thomson, S.N., Gehrels, G.E., Ruiz, J., Buchwaldt, R., 2012. Routine low-damage apatite U–Pb dating using laser ablation-multicollector-ICPMS. Geochem. Geophys. Geosyst. 13, Q0AA21. http://dx.doi.org/10.1029/2011GC003928.
Trotter, J.A., Eggins, S.M., 2006. Chemical systematics of conodont apatite determined by laser ablation ICPMS. Chem. Geol. 233, 196–216.
Tyrrell, S., Haughton, P.D.W., Daly, J.S., Kokfelt, T.F., Gagnevin, D., 2006. The use of the common Pb isotope composition of detrital K-feldspar grains as a provenance tool and its application to Upper Carboniferous paleodrainage, northern England. J. Sediment. Res. 76, 324–345.
Vroon, P.Z., van der Wagt, B., Koornneef, J.M., Davies, G.R., 2008. Problems in obtaining precise and accurate Sr isotope analysis from geological materials using laser ablation MC-ICPMS. Anal. Bioanal. Chem. 390, 465–476.
Waight, T., Baker, J., Peate, D., 2002. Sr isotope ratio measurements by double-focusing MC-ICP-MS: techniques, observations and pitfalls. Int. J. Mass Spectrom. 221, 229–244.
Wasserburg, G.J., Jacobsen, S.B., DePaolo, D.J., McCulloch, M.T., Wen, T., 1981. Precise determination of Sm/Nd ratios, Sm and Nd isotopic abundances in standard solutions. Geochim. Cosmochim. Acta 45, 2311–2323.
Weis, D., Kieffer, B., Maerschalk, C., Barling, J., Jong, J.D., Williams, G.A., Hanano, D., Pretorius, W., Mattielli, N., Scoates, J.S., Goolaerts, A., Friedman, R.M., Mahoney, J.B., 2006. High-precision isotopic characterization of USGS reference materials by TIMS and MC-ICP-MS. Geochem. Geophys. Geosyst. 7, Q08006. http://dx.doi.org/10.1029/2006GC001283.
Willigers, B.J.A., Baker, J.A., Krogstad, E.J., Peate, D.W., 2002. Precise and accurate in situ Pb–Pb dating of apatite, monazite, and sphene by laser ablation multiple-collector ICP-MS. Geochim. Cosmochim. Acta 66, 1051–1066.
Woodhead, J.D., Hergt, J.M., 2001. Strontium, Neodymium and Lead isotope analyses of NIST glass certified reference materials: SRM 610, 612, 614. Geostandards and Geoanalytical Research 25 (2–3), 261–266.
Woodhead, J., Hergt, J., 2005. A preliminary appraisal of seven natural zircon reference materials for in situ Hf isotope determination. Geostandards and Geoanalytical Research 29, 183–195.
Woodhead, J., Swearer, S., Hergt, J., Maas, R., 2005. *In situ* Sr-isotope analysis of carbonates by LA-MC-ICP-MS: interference corrections, high spatial resolution and an example from otolith studies. J. Anal. At. Spectrom. 20, 22–27.

Wu, F.Y., Yang, Y.H., Xie, L.W., Yang, J.H., Xu, P., 2006. Hf isotopic compositions of the standard zircons and baddeleyites used in U–Pb geochronology. Chem. Geol. 234, 105–206.

Wu, F.Y., Yang, Y.H., Bellatreccia, F., Mitchell, R.H., Li, Q.L., 2010a. *In situ* U–Pb and Sr–Nd–Hf isotopic investigations of zirconolite and calzirtite. Chem. Geol. 277, 178–195.

Wu, F.Y., Yang, Y.H., Michael, A.W.M., Liu, Z.C., Zhou, Q., Ge, W.C., Yang, J.S., Zhao, Z.F., Mitchell, R.H., Markl, G., 2010b. *In situ* U–Pb, Sr, Nd and Hf isotopic analysis of eudialyte by LA-(MC)-ICP-MS. Chem. Geol. 273, 8–34.

Wu, F.Y., Yang, Y.H., Mitchell, R.H., Li, Q.L., Yang, J.H., Zhang, Y.B., 2010c. *In situ* U–Pb age determination and Nd isotopic analysis of perovskites from kimberlites in southern Africa and Smoerset Island, Canada. Lithos 115, 205–222.

Wu, F.Y., Yang, Y.H., Li, Q.L., Mitchell, R.H., Dawson, J.B., Brandl, G., Yuhara, M., 2011. *In situ* determination of U–Pb ages and Sr–Nd–Hf isotopic constraints on the petrogenesis of the Phalaborwa carbonatite Complex, South Africa. Lithos 127, 309–322.

Wu, F.Y., Arzamastsev, A.A., Mitchell, R.H., Li, Q.L., Sun, J., Yang, Y.H., Wang, R.C., 2013a. Emplacement age and Sr–Nd isotopic compositions of the Afrikanda alkaline ultramafic complex, Kola Peninsula, Russia. Chem. Geol. 353, 210–229.

Wu, F.Y., Mitchell, R.H., Li, Q.L., Sun, J., Liu, C.Z., Yang, Y.H., 2013b. In situ U–Pb age determination and Sr–Nd isotopic analyses of perovskite from the Premier (Cullinan) kimberlite, South Africa. Chemical Geology. 353, 83–95.

Xie, L.W., Zhang, Y.B., Zhang, H.H., Sun, J.F., Wu, F.Y., 2008. *In situ* simultaneous determination of trace elements, U–Pb and Lu–Hf isotopes in zircon and baddeleyite. Chin. Sci. Bull. 53, 1565–1573.

Yang, Y.H., Sun, J.F., Xie, L.W., Fan, H.R., Wu, F.Y., 2008. *In situ* Nd isotopic measurement of natural geological materials by LA-MC-ICPMS. Chin. Sci. Bull. 53, 1062–1070.

Yang, Y.H., Wu, F.Y., Wilde, S.A., Lui, X.M., Zhang, Y.B., Xie, L.W., Yang, J.H., 2009a. *In situ* perovskite Sr–Nd isotopic constraints on the petrogenesis of the Ordovician Mengyin kimberlites in the North China Craton. Chem. Geol. 264, 24–42.

Yang, Y.H., Wu, F.Y., Xie, L.W., Yang, J.H., Zhang, Y.B., 2009b. *In situ* Sr isotopic measurement of natural geological samples by LA-MC-ICP-MS (in Chinese with English abstract). Acta Petrol. Sin. 25, 3431–3441.

Yang, Y.H., Wu, F.Y., Xie, L.W., Zhang, Y.B., 2010a. High-precision measurements of the $^{143}Nd/^{144}Nd$ isotope ratio in certified reference materials without Nd and Sm separation by multiple collector inductively coupled plasma mass spectrometry. Anal. Lett. 43, 142–150.

Yang, Y.H., Zhang, H.F., Chu, Z.Y., Xie, L.W., Wu, F.Y., 2010b. Combined chemical separation of Lu, Hf, Rb, Sr, Sm and Nd from a single rock digest and precise and accurate isotope determinations of Lu–Hf, Rb–Sr and Sm–Nd isotope systems using multi-collector ICP-MS and TIMS. Int. J. Mass Spectrom. 290, 120–126.

Yang, Z.P., Fryer, B.J., Longerich, H.P., Gagnon, J.E., Samson, I.M., 2011a. 785 nm femtosecond laser ablation for improved precision and reduction of interferences in Sr isotope analyses using MC-ICP-MS. J. Anal. At. Spectrom. 26, 341–351.

Yang, Y.H., Chu, Z.Y., Wu, F.Y., Xie, L.W., Yang, J.H., 2011b. Precise and accurate determination of Sm, Nd concentrations and Nd isotopic compositions in geological samples by MC-ICP-MS. J. Anal. At. Spectrom. 26, 1237–1244.

Yang, Y.H., Wu, F.Y., Xie, L.W., Yang, J.H., Zhang, Y.B., 2011c. High-precision direct determination of the $^{87}Sr/^{86}Sr$ isotope ratio of bottled Sr-rich natural mineral drinking water using multiple collector inductively coupled plasma mass spectrometry. Spectrochim. Acta B At. Spectrosc. 66, 656–660.

Yang, Y.H., Wu, F.Y., Liu, Z.C., Chu, Z.Y., Xie, L.W., Yang, J.H., 2012. Evaluation of Sr chemical purification technique for natural geological samples using common cation-exchange and Sr-specific extraction chromatographic resin prior to MC-ICP-MS or TIMS measurement. J. Anal. At. Spectrom. 27, 516–522.

Yang, Y.H., Wu, F.Y., Chu, Z.Y., Xie, L.W., Yang, J.H., 2013. High-precision simultaneous determination of $^{147}Sm/^{144}Nd$ and $^{143}Nd/^{144}Nd$ ratios in Sm–Nd mixtures using multi-collector inductively coupled plasma mass spectrometry and its comparison to isotope dilution analysis. Spectrochim. Acta B At. Spectrosc. 79 (80), 82–87.

Yang, Y.H., Wu, F.Y., Li, Y., Yang, J.H., Xie, L.W., Liu, Y., Zhang, Y.B., Huang, C., 2014a. In situ U–Pb dating of bastnaesite by LA-ICP-MS. J. Anal. At. Spectrom. 29, 1017–1023.

Yang, Y.H., Wu, F.Y., Xie, L.W., Chu, Z.Y., Yang, J.H., 2014b. Reinvestigation of doubly charged ion of heavy rare earth elements interferences on Sr isotopic analysis using multi-collector inductively coupled plasma mass spectrometry. Spectrochim. Acta B At. Spectrosc. 97, 118–123.

Zaitsev, A., Bell, K., 1995. Sr and Nd isotope data of apatite, calcite and dolomite as indicators of source, and the relationships of phoscorites and carbonatites from the Kovdor massif, Kola peninsula, Russia. Contrib. Mineral. Petrol. 121, 324–335.

Zhou, Q., 2013. In-situ U–Pb isotopic dating of accessory minerals in meteorites(Ph. D. Dissertation) University of Chinese Academy of Sciences and Institute of geology and geophysics, Chinese Academy of Sciences (Supervisor of Prof. Fu-Yuan WU. Chapter 2: 19–22 (in Chinese with English abstract)).

Zhou, H.Y., Liu, D.Y., Nemchim, A., Wan, Y.S., 2007. 3.0 Ga thermo-tectonic events suffered by the 3.8 Ga meta-quartz-diorite in the Anshan area: constraints from apatite SHRIMP U–Th–Pb dating. Geol. Rev. 53, 120–125 (in Chinese with English abstract).

Zhou, H.Y., Geng, J.Z., Cui, Y.R., Li, H.K., Li, H.M., 2012. In situ U–Pb dating of apatite using LA-MC-ICP-MS. Acta Geosci. Sin. 33, 857–864 (In Chinese with English Abstract).